Computer Communications 224 (2024) 254–274

Contents lists available at ScienceDirect

Computer Communications

journal homepage: www.elsevier.com/locate/comcom

Review

Wireless sensing applications with Wi-Fi Channel State Information, preprocessing techniques, and detection algorithms: A survey

Jesus A. Armenta-Garcia, Felix F. Gonzalez-Navarro *, Jesus Caro-Gutierrez

Engineering Institute, Universidad Autónoma de Baja California, Mexicali, Mexico

ARTICLE INFO

Keywords:
Wi-Fi
Channel State Information
Wireless sensing
Wi-Fi sensing

ABSTRACT

Recently, using Wi-Fi devices as sensing technology has garnered significant attention and found numerous applications. This trend has given birth to what is known as Wi-Fi sensing. This innovative approach has been made possible by analyzing the Channel State Information (CSI) of the Wi-Fi communication channel, which can be calculated from the frame preamble. CSI captures multipath effects, attenuations, and phase shifts in signal propagation, among other fading effects caused, for example, by reflection with objects or a person. Extensive research in this field has revealed that these effects can be utilized for sensing purposes, supposing that the cause of the effects is a person, leading to the development of Wi-Fi sensing applications such as Activity Recognition, Gesture Recognition, and Vital Signs monitoring. This Survey highlights recent works and advances in Wi-Fi sensing applications, identifying and exposing significant applications. For each paper selected, the following sections have been emphasized: Data Collection, Data Preprocessing, Detection Algorithm, Performance, and Application, as these are part of the methodology followed for the functioning of Wi-Fi sensing systems. Furthermore, the techniques and tools commonly used in Wi-Fi sensing are described. Finally, the current challenges associated with Wi-Fi as a wireless sensing technology and possible ways to address these challenges are discussed.

1. Introduction

According to the Wi-Fi Alliance, Wi-Fi is the most commonly used wireless communication technology, with approximately 21 billion Wi-Fi devices in use [1]. Although designed for communications, recent works have shown that it can be used for sensing, taking advantage of its ubiquity and resulting in what is known as Wireless Sensing with Wi-Fi Technology, which will be referred to as Wi-Fi sensing in this paper.

Traditional sensing requires a user to use wearable sensors or to have dedicated sensors installed in the sensing area, e.g., accelerometers, smart-watches, or cameras for sensing applications [2–4], regardless of the disadvantages that these imply. Wearable sensors have the disadvantage that the user may need to remember to wear or remove the sensor for various activities, such as bathing, cooking, or device maintenance. Hence, this will result in periods where the user cannot be monitored. In the case of sensors that require installation, such as video surveillance systems, they can only perform the sensing task if the user is within the sensing area or in the line-of-sight (LoS), not to mention that the mere fact that they require installation is a disadvantage, and comes at the cost of the user's privacy [5].

Wireless Sensing systems use either Received Signal Strength (RSS) or Channel State Information (CSI) of the communication channel as measurements to achieve sensing tasks. However, RSS is unsuitable for capturing fine-grained movements, while CSI provides a more detailed description of its surroundings [6], making it the prime option for Wireless Sensing. CSI as a measurement for sensing has been used in several applications such as monitoring breathing rate and heart rate [7,8], fall detection [9], sign language recognition [10], and people identification based on his gait pattern [11]. This paper classifies Wi-Fi sensing systems into nine categories based on their application, which are *Activity Recognition, Gesture Recognition, Vital Signs Monitoring, Indoor Localization, Crowd Counting, Human Pose Estimation, Gait Analysis, Presence Detection, and People Identification*. These categories are described in Section 6, with Fig. 1 illustrating the Wi-Fi sensing systems categories.

In addition to the description, this paper presents the state-of-the-art of each category by highlighting relevant features that lead to the acquisition of results, such as specific scenarios, the hardware used (collecting tool and antenna types), or the detection algorithm employed, as these features are usually emphasized in each work.

* Corresponding author.
E-mail addresses: albany.armenta@uabc.edu.mx (J.A. Armenta-Garcia), fernando.gonzalez@uabc.edu.mx (F.F. Gonzalez-Navarro), jesus.caro@uabc.edu.mx (J. Caro-Gutierrez).

https://doi.org/10.1016/j.comcom.2024.06.011
Received 30 August 2023; Received in revised form 11 June 2024; Accepted 18 June 2024
Available online 27 June 2024

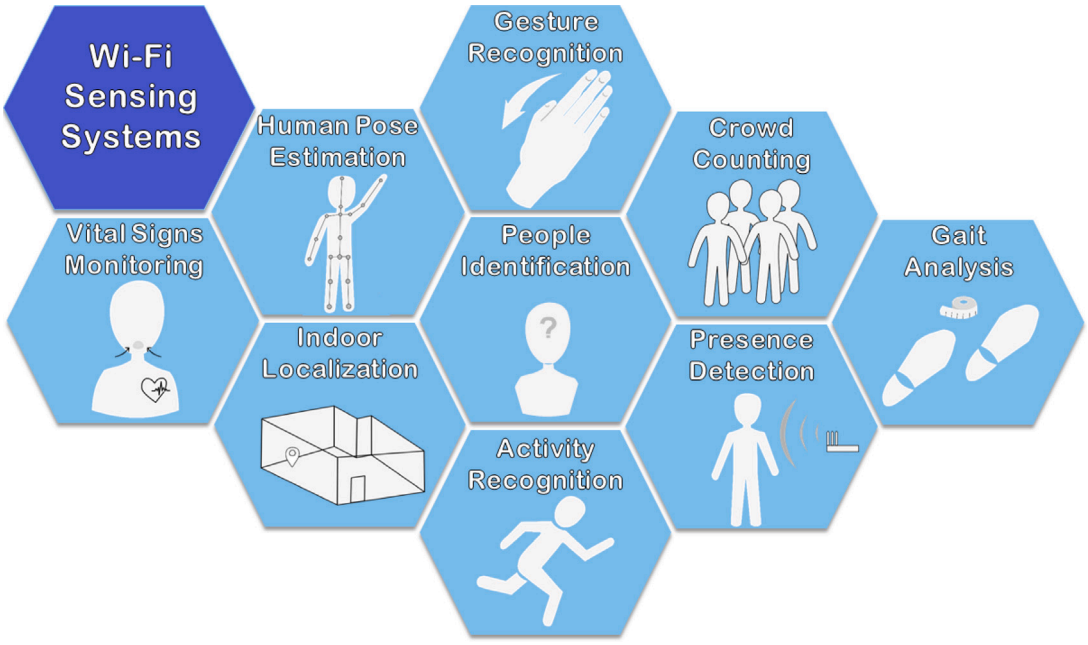

Fig. 1. Wi-Fi sensing systems categories.

The main contributions of this work are:

- A survey about Wi-Fi sensing systems, with the main emphasis on each of the stages of the Wi-Fi sensing methodology.
- A Wi-Fi sensing categories update according to recent work. We present and describe categories not addressed in any other review or survey document.
- We highlight challenges that need to be addressed to improve the performance of Wi-Fi sensing systems.
- Provide a comprehensive Wi-Fi sensing survey that serves as a starting point for new researchers interested in the topic.

The remainder of this paper is organized as follows. Other reviews and surveys related to Wi-Fi sensing systems are presented in Section 2, highlighting their contribution. Then, in Section 3, a description of CSI is provided, as well as tools for collecting CSI from Wi-Fi devices are presented. Using these tools comprehends the first stage of the Wi-Fi sensing systems methodology. Next, in Section 4, CSI Data Preprocessing, commonly used techniques for CSI Data Preprocessing are presented, classifying them into four categories: Noise Reduction, Signal Transform, Dimensionality Reduction, and Feature Extraction. In Section 5, found works are categorized into three different categories according to the detection algorithm used and, thus, by the type of output of the system. These categories are Binary Classification, Multi-class Classification, and Estimation. Section 6 describes each Wi-Fi sensing system category discussed in this paper and each work's contribution. In addition, a summary table is presented for each category to provide an overview of what was done and achieved in each work. In Section 7, current Wi-Fi sensing challenges found through the state-of-the-art are identified: the availability of CSI data, sensing capacity in non-line-of-sight (NLoS) scenarios, data density, the coexistence between communication and sensing, and security. Finally, conclusions are drawn in Section 8.

2. Related work

There are several surveys and literature reviews available on Wi-Fi sensing, but each of them has a different scope. Wi-Fi sensing systems can be analyzed from different points of view since these systems are composed of 4 significant stages that are part of the Wi-Fi sensing methodology, each one of them with its background: CSI Data Collection, CSI Data Preprocessing, Detection Algorithms, and Wi-Fi Sensing Application [12–15]. For example, in a 2019 survey [13], authors provided a complete overview of what Wi-Fi sensing systems consist of, the commonly used preprocessing techniques, the detection algorithms, and the types of applications that could be given to such systems. The categories defined by the authors were Presence Detection, Fall Detection, Motion Detection, Activity Recognition, Gesture Recognition, and People Identification. Moreover, in [16], authors focused on the methodology followed by classification-based Wi-Fi sensing systems, such as Activity Recognition, Gesture Recognition, and Indoor Localization, considering that these systems are composed of the stages of raw CSI preprocessing, feature extraction, and classification. In [17], authors focused on discussing the different types of Wi-Fi Sensing Applications, presenting related work, challenges, and opportunities each type of application has. Lastly, in [18], the topic selected by the authors was the evolution of Wi-Fi sensing over a decade, specifically in Activity and Gesture Recognition and Indoor Localization, establishing that the development of these three types of applications has established milestones in Wi-Fi sensing and that besides its evolution, there are still challenges that need to be addressed.

There have been recent surveys focusing on Wi-Fi sensing methodology. For example, in [12], special attention is given to the detection stage of Wi-Fi sensing systems. The authors highlighted that there are different categories of detection methods, including model-based methods, data-based methods, and model-data hybrid-driven methods. Model-based methods build physical models and transform the CSI into a form that reflects information from the environment for sensing. Data-based methods seek to find hidden attributes in the CSI data to perform prediction, identification, or classification with machine learning models. Model-data hybrid-driven methods preprocess the input that will be used by a machine learning model, resulting in a combination of the categories mentioned above. Similarly, in [15], authors focused on human behavior recognition applications, such as activity and gesture recognition, presence detection, and breathing rate monitoring. In this survey, applications were divided into three different categories: pattern-based applications, which use pattern recognition methods such as machine learning algorithms; model-based applications, which recognize human behavior by utilizing mathematical or physical models

Table 1
Comparative table of related work.

	[13]	[15]	[16]	[17]	[14]	[12]	[19]	[18]	[20]	Our work
Year	2019	2019	2019	2020	2022	2022	2022	2022	2023	2024
CSI description	Yes	Yes	Yes	Yes	Yes	Yes	Yes	Yes	Yes	Yes
Describes available CSI collecting tools	Yes	No	No	No	Yes	Partially	Yes	Yes	No	Yes
Describes the operational methodology of Wi-Fi sensing systems	Yes	Yes	Yes	Yes	Yes	No	Yes	No	Yes	Yes
Sensing applications	AR, GR, PD, PI, VS, IL, and CC	AR, GR, VS, CC, PD, PI	IL, AR, and GR	VS, PI, AR, GR, GA, PD, and IL	VS	PD, AR, CC, IL, PI, and GR	VS, AR, GR, HP, and IL (Healthcare)	AR, GR, and IL	IL, AR, GR, VS, PD, and CC	AR, GR, VS, IL, CC, HP, GA, PD, and PI
Describes the CSI data preprocessing stage	Yes	Yes	Yes	Yes	Partially	No	Yes	No	Yes	Yes
Describes the detection stage	Yes	Yes	Yes	No	Yes	Yes	Yes	No	Yes	Yes
Provides an insight on preprocessing techniques for Wi-Fi sensing	Yes	Yes	No	Yes	No	Yes	Yes	No	Yes	Yes
Proves an insight on detection algorithms for Wi-Fi sensing	Yes	Yes	Yes	Yes	No	Yes	Yes	No	No	Yes
Mention the CSI collecting tool used and antenna types in communication devices	No	No	No	No	No	No	Yes	No	No	Yes
Summarize the results obtained in each presented work	Yes	Yes	Yes	Yes	Yes	Yes	Yes	No	No	Yes

Notes: AR—Activity Recognition, GR—Gesture recognition, VS—Vital signs monitoring, IL—Indoor localization, CC—Crowd Counting, HP—Human pose estimation, GA—Gait Analysis, PD—Presence Detection, PI—People Identification.

that allow to relate CSI variations into human behavior; and deep-learning based applications, which uses deep learning models that do not require manual feature extraction.

In [14], there is a focus on collecting and analyzing state-of-the-art Wi-Fi sensing for monitoring vital signs such as breathing rate, heart rate, or both. The authors presented a guideline for the use of CSI for medical purposes. Similar to this work, in [19], authors presented works about healthcare monitoring systems using CSI, expanding to systems for detecting Parkinson's disease or auxiliary systems such as fall detection systems and even mentioning systems for human pose estimation through CSI. Finally, in [20], the authors described CSI Data Preprocessing techniques for Wi-Fi sensing and how these can be implemented in embedded devices such as microcontrollers.

This paper, unlike the previous ones, aims to provide a comprehensive overview of the methodology stages involved in Wi-Fi sensing systems: *CSI Data Collection, CSI Data Preprocessing, Detection Algorithms, and Wi-Fi Sensing Applications*; and focused on including the most recent Wi-Fi Sensing applications, as over the years Wi-Fi sensing applications have increased due to various efforts made by researchers around the world. These can be noticed in Table 1, where a comparison is presented between related work and this work.

The stages of the methodology and the set of techniques and concepts that compose each stage addressed in this work are presented in Fig. 2.

3. Channel state information

The CSI originates in the physical layer, and its purpose is to mitigate the multipath fading effects of a wireless channel since it allows MIMO-based systems to adapt to the current channel conditions. The Wi-Fi channel can be modeled as

$$y = Hx + \eta \tag{1}$$

where y is the received signal, and x is the transmitted signal plus some noise η. For constructing H, which has the information about the multipath fading present in the channel, amplitude attenuation, and phase shift, the transmitter sends pre-defined symbols, known as Long Training Field symbols (LTFs), for each subcarrier generated by Orthogonal Frequency-Division Multiplexing (OFDM) in each frame preamble [13]. These symbols allow the receiver to estimate channel characteristics, an operation known as channel estimation, which results in the calculation of CSI. In 802.11n, which is the Wi-Fi standard in which the vast majority of Wi-Fi sensing systems are based, a 20 MHz channel is divided by OFDM into 64 subcarriers, where 52 are data subcarriers, 4 are pilot subcarriers used for synchronization purposes between transmitter and receiver, and 8 are unused subcarriers used as guard carriers against interference from adjacent channels, each with a spacing of 312.5 kHz [21]; while Wi-Fi 6, 802.11ax, adopts a 160 MHz channel divided into 2048 subcarriers, which allows finger grained motion detection because of the wider bandwidth [22,23].

For wireless communications, CSI is used to improve the receiving signal strength and throughput in a technique known as beamforming, implemented since 802.11n and now in Wi-Fi 6, with explicit beamforming, where the receiver provides its channel estimates or compressed beamforming weights (for Wi-Fi 6) for beamforming [23, 24].

For Wi-Fi sensing applications, CSI is defined as a collection of matrixes, in which each matrix H is represented as shown in Fig. 3. Each matrix element $H_{n,m,k}$ is a complex number that builds up the Channel Frequency Response for each communication link given by the number of receiver antennas N and of transmitter antennas M for every subcarrier k, and it can be expressed at a time t and given the central frequency f of k as:

$$H_{m,n,f}(t) = \sum_{i=1}^{L} \alpha_i(t) e^{-2j\pi f \tau_i(t)} \tag{2}$$

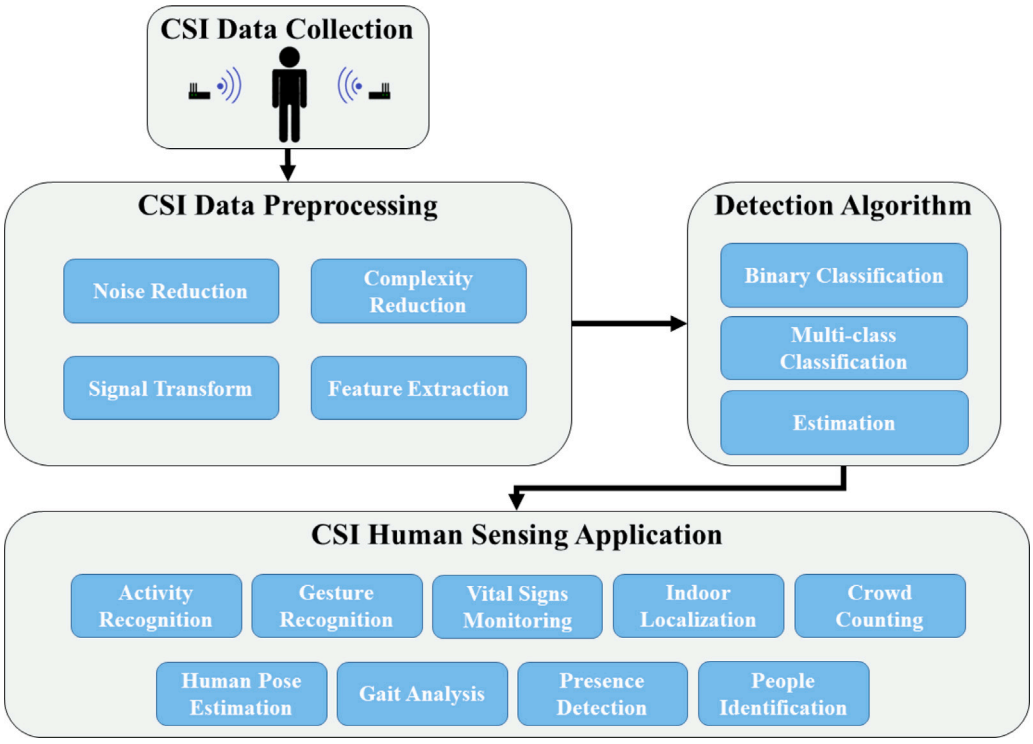

Fig. 2. Operational methodology of Wi-Fi sensing systems.

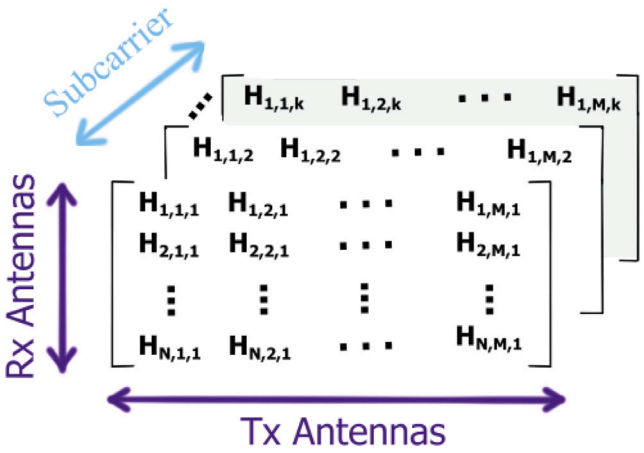

Fig. 3. CSI Matrix representation.

where L is the number of propagation paths due to signal reflections by the presence of objects within the propagation environment, $\alpha_i(t)$ is the attenuation, and $\tau_i(t)$ is the propagation delay of the ith path [25].

As multipath effects are present in CSI, it will gather information on how a Wi-Fi signal behaves in the channel. The presence of surrounding objects or people is part of the indoor channel. Hence, we can infer that the presence of a person or even his actions will result in fluctuations in the Wi-Fi signal transmitted through the indoor channel, leading to what now is known as *Wi-Fi sensing*.

3.1. CSI collecting tools

CSI is physical layer information calculated by commercial Wi-Fi devices. However, it cannot be obtained directly for Wi-Fi sensing applications as current Wi-Fi standards, such as the IEEE 802.11n/ac, do not facilitate the collection of CSI. Thus, over the years, tools have been developed to collect CSI.

One of the most utilized CSI collection tools for Wi-Fi sensing systems is the *Linux 802.11n CSI Tool* [26]. Halperin et al. developed this tool using the Intel 5300 NIC and applying custom firmware. It is available in a well-known repository with all the necessary programs and scripts to collect and analyze CSI data. Each CSI matrix entry reported by this tool has a signed 8-bit resolution for the complex number that can be converted to amplitude attenuation and phase shift. This firmware enables an Intel debugging mode that records CSI from up to the 30 subcarriers available by the chipset for each correctly received 802.11n frame. It sends it to the kernel driver to be passed to a user-space program for processing.

Another CSI collecting tool uses multiple Atheros 802.11 Wi-Fi chipsets, receiving the name of *Atheros CSI Tool* [27]. Unlike the Linux 802.11n CSI Tool, the CSI matrix entry has a 10-bit resolution and reports information from up to 56 subcarriers for a 20 MHz channel and 114 subcarriers for a 40 MHz, depending on the desired configuration of the collecting system. As it is a modified firmware of an open-source Linux kernel, it can work with Linux distributions such as Ubuntu for personal computers and OpenWRT. The latter allows the implementation of this CSI collecting tool in embedded devices, including Wi-Fi routers.

Applications using the previously mentioned monitoring tools have obtained satisfactory results, proving their effectiveness. However, they have two notable limitations: (1) They need one or more laptop or desktop computers equipped with an Intel 5300 NIC for Linux 802.11n CSI Tool or Wi-Fi devices with a compatible chipset for Atheros CSI Tool. This resource limitation may impact the deployment of a large-scale system where it is needed to use low-cost equipment or where space is limited; (2) For Intel 5300 NIC, only 30 out of 52 data subcarriers can be obtained. To overcome this problem, ESP32 CSI Toolkit [28] uses an ESP32 microcontroller that implements the ESP Wi-Fi API for collecting CSI [29]. These devices can act as both an AP or a station under TCP protocol and 802.11b/g/n standards in 20 and 40 MHz channels with support to receiving frames with legacy long training field (LLTF), high throughput LTF (HT-LTF), and space–time block code HT-LTF (STBC-HT-LTF) in the preamble. ESP32 CSI

Table 2
Summary of preprocessing techniques.

Preprocessing purpose	Reference
Noise reduction	Low-pass filter: [10,25,30–50] Multipath removal: [34,51–54] Hampel filter: [7,8,34,40,47,48,54–65] Moving average filter: [7,57,58,62,66–69] Savitzky-Golay filter: [54,57,59–61,70–74] Phase sanitization: [8,10,25,30,55,66,67,73,75–87] MUSIC: [88–91]
Signal transform	FFT: [8,36,43,46,56,68,71,92,93] PSD: [7,57,58,60,94] DWT: [8,31,42,56,57,65,68,95–101]
Complexity reduction	PCA: [7,9,10,31,33,34,36,37,41–43,45,50,54,57,65,69,70,84,95,98,102–110] Variance-based subcarrier selection: [7,52,58,82,97] Signal segmentation: [30,31,47,52,55,70,74,101]
Feature extraction	Manual feature extraction: [7,10,31–34,40–42,45,53–55,61,62,65,71,75,82,89,95,96,101,103–105,107–109,111–113] Automatic feature extraction: [9,11,25,30,35,37–39,44,46,48,50,65,67,69,74,76–81,83,84,87,97–100,102,106,110,114–124]

Toolkit can obtain CSI amplitude and phase shift from 64 subcarriers, and by using a microcontroller, ESP32 CSI Toolkit results in a flexible, low-cost, and easy-to-deploy tool for Wi-Fi sensing applications.

Nexmon CSI extractor [125,126] is a C-based firmware patching framework for Broadcom and Cypress Wi-Fi chips that allows collecting CSI. It is compatible with Wi-Fi 802.11a/n/ac standards with up to 80 MHz channel bandwidth and 256 subcarriers' information, supporting VHT PHY and 4 × 4 MIMO. This tool supports devices such as the Raspberry PI platform and smartphones, and it comes with an application that allows us to set up the Wi-Fi chip according to our needs, capture CSI, and observe a dynamic heat map plot representing CSI values' magnitude. Recently, Nexmon CSI has been ported and adapted to the Broadcom 43 684 chipset, supporting the high efficiency (HE) PHY introduced in 802.11ax, with bandwidth up to 160 MHz and 4 × 4 MIMO, where each channel is divided into 2048 subcarriers. This milestone allows obtaining information from 32 768 subcarriers in a 4 × 4 MIMO system [127].

Openwifi [128] is a free and open-source Software Defined Radio (SDR) implementation that currently supports 802.11 a/g/n Wi-Fi standards, with 802.11ax support under development. Openwifi is based on Xilinx Zynq System on Chip (SoC), which consists of a Field-Programmable Gate Array (FPGA) and an ARM processor embedded with Linux and with an SDR driver for interacting with the SDR implemented in the FPGA, where low MAC and PHY are also implemented. For CSI collecting, CSI data is generated in the FPGA and then passed to the Linux kernel and user space in the SDR board, from where CSI can be extracted for processing or visualization to a computer by connecting an Ethernet cable to the board, being able to collect data from 56 subcarriers under 802.11n.

Besides these tools, there are ongoing efforts to develop a new standard amendment for Wi-Fi sensing called IEEE 802.11bf. This amendment aims to enhance the capabilities of Wi-Fi sensing and facilitate the deployment of Wi-Fi sensing systems without requiring additional tools for CSI collection [129].

4. CSI data preprocessing

Once CSI data is collected, it is necessary to apply a preprocessing step to extract useful information from it as freely as possible from noise and in a format suitable for detection algorithms. This section will present multiple techniques commonly used in this step, which accomplish one of the following tasks: *Noise Reduction, Signal Transform, Dimensionality Reduction* and *Feature Extraction*. Table 2 lists the most common preprocessing techniques found in the state-of-the-art and relates them to existing works.

4.1. Noise reduction

As Wi-Fi is an electromagnetic signal, it is susceptible to multiple noise sources, e.g., other Wi-Fi signals or devices, the movement of objects, and the presence of people near the sensing area, which affect the quality of CSI data. Noise Reduction techniques are intended to mitigate the effects of these noise sources. For example, Fig. 4 shows the result of applying a low-pass filter and a Savitzky–Golay filter to raw CSI amplitude data.

Some commonly used Noise Reduction techniques in the Wi-Fi sensing literature are:

1. *Low-pass filter:* a filter that allows all frequencies up to a cut-off frequency f_c, where frequencies above this are attenuated. At f_c, the filter response curve presents an attenuation of −3 dB concerning the magnitude presented in the pass-band region of the filter [130]. This filter is used to remove high-frequency noise that interferes with the sensing application.
2. *Multipath removal:* a Power Delay Profile (PDP) profiles the multipath arrivals of the signals as a function of propagation delay. CSI represents the channel's frequency response so it can be transformed to the time domain PDP through an Inverse Fast Fourier Transform [22]. Multipath Removal based on PDP consists of removing those multipath components with a delay higher than 500 ns, as it is the maximum propagation delay incurred by a reflected path for an indoor environment [51].
3. *Hampel filter:* it is used to identify and replace outliers of CSI databases on the median m and the median absolute deviation. An entry x_i will be considered an outlier if the condition $|x_i - m| > tS$ is met, where $S = 1.4826 \times median(|x - m|)$ and t is a configurable threshold value for outlier detection [131].
4. *Moving Average filter:* this filter can be seen as a simple low-pass filter to smooth CSI data while reducing random noise. It takes M samples of the signal, known as a *window* of a signal x [132]. These values are used to produce an output signal y defined as

$$y[n] = \frac{1}{M} \sum_{k=0}^{M-1} x[n-k] \tag{3}$$

5. *Savitzky–Golay filter:* this filter can also be seen as a low-pass filter, which smooths data based on local least-squares polynomial approximation, reducing noise while maintaining the shape and height of waveform peaks. Suppose having a signal f, for each time step, $f(t)$ is replaced by the value obtained by fitting a polynomial $\hat{f}(i)$ to f on time steps between two intervals defined by the filter's window size. This is done by least-squares polynomial fitting using convolution [133].

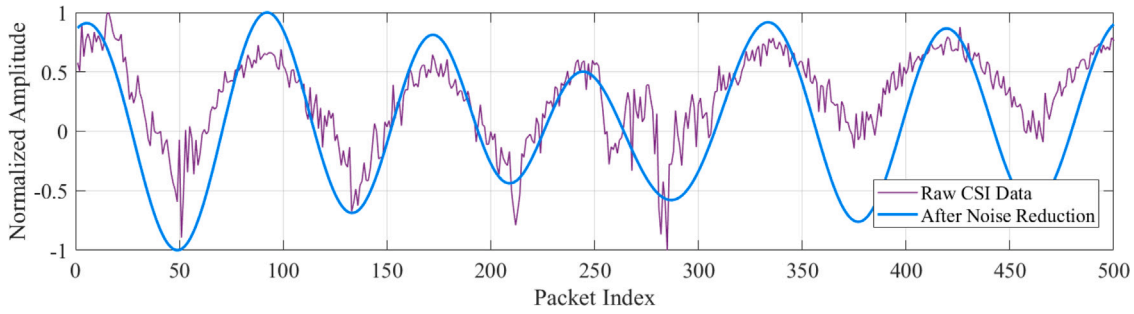

Fig. 4. Result of applying filters to raw CSI Data.

6. *MUSIC algorithm:* Multiple Signal Classification (MUSIC) algorithm [134] is based on the idea that incident signals with different incident angles cause different phase changes on each antenna [88]. In an antenna array, the distance between adjacent antennas is d, and the angle-of-arrival (AoA) is θ. Assuming that propagation paths are longer than θ, the path difference between adjacent antennas is $dsin(\theta)$ and leads to a phase difference of $-2\pi f dsin(\theta)/c$, where f is the signal frequency and c the speed of light. Thus, phase difference Φ can be denoted as a function of the AoA:

$$\Phi = e^{-j2\pi f dsin(\theta)/c} \tag{4}$$

and phase difference of the antenna array can be defined as

$$a(\theta) = [1, \Phi(\theta), \ldots, \Phi(\theta)^{M-1}]^T \tag{5}$$

where M is the number of antennas in the antenna array and $a(\theta)$ is known as the steering vector. If signal $s(t)$ is received at the first antenna, the signal at the i-th antenna can be expressed as

$$x_i(t) = \Phi(\theta)^{i-1} s(t) + n_i(t) \tag{6}$$

and the received signal vector as

$$X(t) = [x_1(t), \ldots, X_M(t)]^T = a(\theta)s(t) + N(t) \tag{7}$$

where $n_i(t)$ is the noise of the signal received at the i-th antenna and N the noise vector.
When there are n incident signals at the array, the received signal $s(t)$ is the superposition of all incident signals, and therefore the received signal vector can be expressed as:

$$X(t) = \sum_{i=1}^{n} a(\theta_i)s_i(t) + N(t) = AS(t) + N(t) \tag{8}$$

The MUSIC algorithm performs eigenstructure analysis on the correlation matrix R_x of the received signal X. R_x, which has M eigenvalues can be defined as

$$\begin{aligned} R_x &= E[XX^H] \\ &= A\mathbb{E}[SS^H]A^H + \mathbb{E}[NN^H] \\ &= AR_sA^H + \sigma^2 I \end{aligned} \tag{9}$$

where R_s is the correlation matrix of the signal vector. In practice, the correlation matrix is obtained as [88]

$$\hat{R}_x = \frac{1}{L}\sum_{i=1}^{L} XX^H \tag{10}$$

The eigenvectors with the smallest $M-n$ eigenvalues construct a noise vector subspace E_N, and the rest n eigenvectors construct a signal subspace E_s. As these subspaces are orthogonal, the spatial spectrum is defined by equation

$$P(\theta)_{MUSIC} = \frac{1}{a^H(\theta)E_N E_N^H a(\theta)} \tag{11}$$

In Wi-Fi sensing systems, the MUSIC algorithm is used to find the paths reflected by the target of interest for sensing with variations to traditional MUSIC algorithm as can be seen in [88–90].

7. *Phase Sanitization:* as CSI phase is not often used because of measurement errors induced in the transmission process due to hardware imperfections. Three of these errors that are commonly treated in the literature are the Sampling Frequency Offset (SFO), the sampling frequencies of the transmitter–receiver exhibit an offset due to non-synchronized clocks, Packet Boundary Detection (PBD), caused by the sensitivity of packet detector, and Central Frequency Offset (CFO), as the central frequencies of the transmitter–receiver cannot be perfectly synchronized [22]. Three common methods to treat with these errors in the literature are the use of phase difference between adjacent antennas [8,30,55,66,75–81], linear transformation/fitting [10,67,82], and conjugate multiplication [25,83,84].

4.2. Signal transform

Sometimes it is necessary to transform CSI data to a domain other than time to obtain additional information about what CSI is capturing about the surroundings, e.g., transforming CSI data to the frequency domain would allow us to observe the frequency of periodic variations occurring in the CSI, which may represent a movement that is being performed periodically by a person. In literature, it is common to find that tools are being used to transform data to the frequency domain or to a time–frequency representation, such as the following:

1. *Fast Fourier Transform (FFT):* the Fourier Transform is a tool that allows us to observe how a signal x consists of a sum of complex exponentials at different frequencies, allowing us to obtain what is known as the frequency domain of the signal. The FFT is a version of the Discrete Fourier Transform to be implemented in software to analyze the frequency properties of a signal, as it reduces the calculations done by the computer and, therefore, reduces computational complexity [135].
2. *Power Spectral Density (PSD):* it is a tool that describes the distribution of signal frequency components by representing the proportion of the total signal power contributed by each frequency component. The PSD, or spectrum for short, is obtained by multiplying each frequency bin obtained with FFT by its complex conjugate, which results in a squared amplitude that is then normalized to the width of the frequency bin [136].
3. *Discrete Wavelet Transform (DWT):* a wavelet is an oscillating orthogonal function of time or space used as a window function with finite duration and zero mean, used as a tool for the analysis of transient, non-stationary, or time-varying phenomena [137]. The wavelet transform consists of decomposing an input signal from functions derived from a selected wavelet named the

mother wavelet ψ. These derivatives are obtained by scaling and shifting ψ and can be defined as

$$\psi_{(a,b)}(t) = \frac{1}{\sqrt{a}}\psi\left(\frac{t-b}{a}\right) \tag{12}$$

where a refers to the scaling factor and b to the shift factor. Thus, the wavelet transform can be defined as a decomposition of a signal $s(t)$ into a set of scaled and shifted wavelet functions $\psi_{(a,b)}(t)$ constructing a time–frequency description of $s(t)$ [138]. This definition can be expressed as

$$T(b,a) = \frac{1}{\sqrt{a}}\int \psi\left(\frac{t-b}{a}\right) s(t)dt \tag{13}$$

In the DWT, both a and b are discretized, specifically a is discretized along the sequence 2^j, where j is a positive integer value [139]. When computed, the DWT is achieved by multilevel decomposition, passing the input signal through a low-pass and high-pass filter in parallel. These filters are defined according to the selected ψ. The output from the high-pass filter is referred to as detail coefficients and maintains the high-frequency components of the input signal. In contrast, low-frequency components are obtained from the low-pass filters, and these are called approximation coefficients. The decomposition process is iterative and repeated depending on the DWT level selected. At each level, the approximation coefficients obtained in the previous level are filtered by the same high-pass and low-pass filters [140].

4.3. Dimensionality reduction

It is important to note that subcarriers capture different types of information due to multipath propagation. This means that some subcarriers may capture relevant information for a particular task, while others may not. That is why Wi-Fi CSI sensing systems attempt to retain only useful information, generate a reliable response, and reduce the processing time by reducing the amount of information to be processed. Among the articles selected for this survey, two methods for dimensionality reduction stand out: *Principal Component Analysis (PCA) and Variance-based Subcarrier Selection*, while Signal Segmentation techniques are also implemented.

1. *PCA:* is a statistical technique used for reducing the dimensionality of a dataset by finding new uncorrelated variables, namely Principal Components (PC), which are linear combinations of the original variables of the dataset [141].
2. *Variance-based Subcarrier Selection:* it is the most common subcarrier selection algorithm found in the literature because of its simplicity and effectiveness. It is based on experimental results that have shown that subcarriers with high variance value in M CSI data samples are more prone to containing relevant information for sensing applications [7,52,75,82].
3. *Signal Segmentation:* this stands for a group of techniques that focus on finding the start or ending point of a specific event, e.g., breathing or activity, only to retain a time window of the signal enclosed by these points [31,52,70]. Signal Segmentation techniques might reduce the amount of data to be processed and increase the system's performance as only the relevant signal window is used to achieve sensing.

4.4. Feature extraction

Feature Extraction involves performing an additional transformation of the raw or preprocessed CSI data to generate features that will serve as inputs for the machine learning algorithms. These features can be extracted manually, i.e., the authors decide which features will be used as input and can usually be obtained from the time or frequency domain of the CSI data. In these features, we can find the mean, median, standard deviation, and frequency with the most significant magnitude of the spectrum, among others [32–34,82]. Alternatively, features can also be extracted automatically by deep learning techniques responsible for the detection [35,114].

5. Detection algorithm

For this article, the commonly used detection algorithms for Wi-Fi sensing systems are categorized according to the type of system response: *binary classification, multi-class classification, or estimation*. Table 3 shows the articles discussed in this work according to the developed system response.

5.1. Binary classification

This category, together with *Multi-class Classification*, arises from observing that machine learning algorithms for classification are commonly used in Wi-Fi sensing systems, and one way to categorize these is according to their type of response. The binary classification consists of machine learning algorithms that classify an observation into one of two possible classes. This type of response is commonly seen in Presence Detection systems, where the system detects whether or not a person is present in the room [96,142].

5.2. Multi-class classification

In addition to Binary Classification, machine learning algorithms can classify an observation into one of three or more classes are called Multi-class Classification Algorithms. A clear example of Wi-Fi sensing systems whose Detection Algorithm falls under this category are Activity or Gesture Recognition systems, as they identify a specific action between three or more registered actions, such as in [32] where they used k-NN and SVM machine learning algorithms to recognize between running, walking, and hand moving, or as in [40] were k-NN algorithm is used to recognize between 9 different finger gestures.

5.3. Estimation

Wi-Fi sensing systems with an estimation-based detection algorithm show a continuous magnitude calculated from CSI characteristics instead of performing classification and do not require an offline phase in which known data are used to train an algorithm, except for those that use machine learning algorithms for regression. In this category are, for example, systems used to monitor vital signs, in which peak detection algorithms or frequency spectrum analysis using the FFT are commonly used to estimate breathing rate [51,92].

6. Wireless human sensing applications using CSI

6.1. Activity recognition

As its name suggests, Human Activity Recognition focuses on recognizing daily human activities in real-life settings based on a predefined activity model [146]. For this paper, an activity is defined as a human action involving a change of total body position or multiple body parts simultaneously that could involve a daily activity, e.g., walking, running, or eating.

The importance of activity recognition lies in the fact that it can be applied in myriad Internet of Things applications, e.g., to identify if an older adult suffered a fall and, therefore, notify the health services; in smart homes, to define daily activity patterns; and even in sports, to know if an exercise is performed correctly.

Table 3
Summary of collected wireless sensing applications.

Response type	Sensing application
Binary classification	Activity recognition: [9,143] People identification: [98] Presence detection: [49,62,81,96,99,103,110,142,144]
Multi-class classification	Activity recognition: [25,32,33,36–38,42,50,69,74,87,95,100,101,106,107,114,120]; Sleep postures: [7,56] People identification: [11,31,42,44,45,53,54,85,104,105] Gait analysis: [102] Gesture recognition: [10,30,34,35,39–41,69,71,72,76,77,84,89,108,118] People counting: [48,55,63,79,90,96,117,119] Vital signs monitoring: [46,82] Indoor localization: [80,109,111,112,122,123] Human pose estimation: [97,115]
Estimation Frequency analysis, Peak detection, Regression, MUSIC algorithm, Correlation, Genetic algorithms	Gait analysis: [43,60,143] Human pose estimation: [83,116,124] Vital signs: [7,47,51,56–59,64,66,68,70,71,90,92,94] Gesture recognition: [73] People counting: [61,67,75,93] Indoor localization: [78,86,88,91,113,121,145]

6.1.1. CSI activity recognition related work

In [9], they propose using CSI spectrogram images for fall detection. This same activity was identified in [143], where, unlike the previous one, they generated a mathematic model to determine if the person suffered a fall. Fall detection is commonly accompanied by the detection of other activities, e.g., walking or sitting [33,38,95,107]. For example, TW-See [33] is a system that extracts attributes from the CSI amplitude, which are then used as input to a neural network that can identify from among seven different activities: no activity, walking, hand swing, falling, sitting down, boxing and standing up; achieving an accuracy of 90.54% even though a concrete wall separated the Wi-Fi device and the person to be monitored. On the other hand, in [38], they used up to 4 Wi-Fi communication devices to identify no activity: walking, cooking, eating, bathing, using the toilet, sleeping, and falling. It is essential to notice that these are activities performed in different rooms, and despite this, they achieved accuracy values above 96%.

In [95], they used a statistical model known as the Hidden Markov Model for activity recognition from a set of 11 daily activities, such as brushing teeth and opening the refrigerator can be found, achieving an accuracy of 72%. This same model was used in [42] to recognize no activity, sitting down, pushing, hand swinging, and waving.

The authors in [107] developed a system to identify between walking, sitting down, lying, standing up, squatting down, and crawling activities in LoS and NLoS scenarios, presenting accuracies above 91% in both scenarios utilizing a Random Forest classifier. Classification algorithms, such as k-NN and SVM, were used in [32] to identify whether a person is running, walking, or moving a hand. In addition, they implement an algorithm that allows them to identify the start and the end of an activity as in [36,37]. Meanwhile, authors in [101] compared the performance of 3 different classifiers, Random Forest, Gradient Boosting, and Extreme Gradient Boosting, for activity recognition with CSI collected from ESP32 in sniffer mode, obtaining a cross-validation accuracy of 83.39%.

Deep Learning has been used for activity recognition, such as the case of [120], where they used a Convolutional Neural Network (CNN) and Long Short-Term Memory (LSTM) for the detection of 6 different activities, achieving a cross-validation accuracy of 97.6%. An LSTM was also used in [5] to compare if its performance with no sophisticated preprocessing could be as good as with SVM with noise reduction, dimensionality reduction, and feature extraction. The authors found that in a LoS scenario, the LSTM outperforms the SVM approach. Nonetheless, in [65], authors obtained similar performance results between an SVM and LSTM model for activity recognition of 8 activities in a LoS scenario, but highlighting that careful data preprocessing steps are needed to achieve similar performance with the SVM. In [114], they used a CNN to extract features from raw CSI data, which an ensemble classifier will use later. With this approach, they obtain an accuracy of 98.9% for identifying the activities of sitting down, jumping, waving, picking up, walking, and running. In [106], they employed algorithms for creating synthetic CSI data to improve activity detection performance, achieving an improvement of up to 34.6% and an accuracy of about 89% for the identification of ten different activities by using a Dense-LSTM. Other CNN models were utilized in [25,74], obtaining accuracies of 95% and above 89%, respectively. The latter focused on identifying activities that were done one after the other in a time series, as they would be performed daily with the implementation of a Temporal Convolutional Network (TCN), which exhibits a more extended memory if compared to other network architectures such as long short-term memory (LSTM), making TCNs more suitable for daily activity monitoring. A drawback stated by authors in [100] is that the model training is usually done a single time, preventing the model from being able to learn new activities. That is why they developed a Deep Learning model based on incremental Learning by creating four scenes with different activities from each other, which are later used in training iterations for updating the model. They obtained that when the fourth scene is introduced in the model, it can identify up to 17 activities with an accuracy of 92.8%. SHARP [87] is an activity recognition system designed for changing scenarios that uses multiple CNNs, one for data collected from each antenna, for obtaining one activity vector from each communication link. These vectors are later fused to recognize the activity, obtaining an average accuracy of 96% in scenarios different from training. Moreover, in [50], a gated temporal CNN with residual connections that takes as input CSI tensors built from CSI matrices was used for recognizing up to 8 activities in a different scenario from training. Authors observed that their approach performs better under changing scenarios than traditional CNNs and LSTMs, with a cross-domain accuracy of 97.57%. Finally, in [69], they used a Dense Neural Network architecture to identify activities related to physical therapy and gym equipment activities, obtaining an accuracy above 80.65% and 93%, respectively, collecting CSI with ESP32 microcontrollers.

The performance and activities detected in each presented work are summarized in Table 4.

6.2. Gesture recognition

Unlike activity recognition, gesture recognition focuses on smaller-scale actions that do not involve a position change, such as finger, hand, and mouth movements. The literature refers to these movements as gestures.

There are many articles stating that gesture recognition plays a vital role in Human–Computer Interaction [10,35,76,77] as it can be used to interact with a myriad of applications without the need for a control device, e.g., virtual reality systems, smart home control, and sign language recognition.

Table 4
Activity recognition applications.

Reference	Activities	Collecting tool	Communication hardware	Performance
[5]	Walk, run, sit, stand, and empty/no activity.	Linux 802.11n CSI Tool	Tx-1 antenna, Rx-3 antennas, type not specified	Accuracies ≥ 95%, LSTM outperforms SVM in LoS scenario.
[9]	Falling	Linux 802.11n CSI Tool	Antenna array	90% accuracy.
[25]	Walk, hand movements, jump, box, sit down, and sit up	Linux 802.11n CSI Tool	Tx-1 OMNI antenna, Rx-3 OMNI antennas	Accuracies ≥ 89%.
[32]	Running, walking, and hand moving	Linux 802.11n CSI Tool	Tx-3 OMNI antennas, Rx-1 OMNI antenna	Accuracies ≥ 89.2%.
[33]	No activity, walk, hand swing, fall, sit down, boxing, and stand up	Linux 802.11n CSI Tool	Tx-1 OMNI antenna, Rx-3 OMNI antennas	90.54% accuracy.
[114]	Sit down, jump, wave, pick up, walk, and run	Atheros CSI Tool	Tx-1 OMNI antenna, Rx-3 OMNI antennas	98.9% accuracy.
[36]	Dumbbell lifting, deep squat, kicking, and boxing	Linux 802.11n CSI Tool	Tx-3 OMNI antennas, Rx-1 OMNI antenna	97.8% accuracy.
[37]	3 literature activity datasets	Linux 802.11n CSI Tool	Tx-2 OMNI antennas, Rx-3 OMNI antennas	Accuracies ≥ 97.5%.
[38]	No activity, walk, cook, eat, bathe, use toilet, sleep, and fall	Linux 802.11n CSI Tool	Not specified	Accuracies ≥ 96%.
[42]	No activity, walk, sit down, push, swing, and wave	Linx 802.11n CSI Tool	Tx-2 OMNI antennas, 2 Rx-3 OMNI antennas	92.9% accuracy.
[50]	Fall, walk, run, sit down, stand up, jump, wave hand, and stoop	Linux 802.11n CSI Tool	not specified	97.57% accuracy.
[95]	Run, walk, sit down, open refrigerator, fall, box, push one hand, brush teeth, and no activity	Linx 802.11n CSI Tool	Not specified	72% accuracy.
[100]	17 activities, such as stretch, jump, and sit down	Linux 802.11n CSI Tool	Not specified	92.8% accuracy.
[101]	Empty, walk, sit down, and stand up	ESP32 CSI Toolkit	Single onboard antenna	83.39% cross-validation accuracy.
[69]	Physical therapy activities and use of gym equipment	ESP32 CSI Toolkit	Single onboard antenna, up to 3 ESP32 as Rx	Accuracy > 80%.
[74]	WiAr dataset [147]	Linux 802.11n CSI Tool	Tx-1 OMNI antenna, Rx-3 OMNI antennas	95% accuracy.
[87]	Empty, walk, run, sit down, and jump	Nexmon	Tx-1 antenna, Rx-4 antennas, type not specified	96% accuracy in changing environments.
[106]	Phone call, check wristwathc, walk, walk fast, run, jump, lie down, play guitar, play piano, and play basketball	Atheros CSI Tool	Tx and Rx-3 OMNI antennas	89% accuracy.
[107]	Walk, sit down, lie, stand up, squat down, fall, and crawl	Linux 802.11n CSI Tool	Tx-2 OMNI antennas, Rx-3 OMNI antennas	95.43% accuracy for LoS scenario, and 91.2% for NLoS scenario.
[120]	No activity, sit, walk, lie, run, and stand	OpenWrt firmware	Transceivers with 3 OMNI antennas	97.6% cross-validation accuracy.
[143]	Falling	Linux 802.11n CSI Tool	Tx-2 OMNI antennas, Rx-3 OMNI antennas	95% accuracy.

6.2.1. CSI gesture recognition related work

One application for gesture recognition is the identification of finger and hand gestures, as demonstrated in [40], a system was developed to identify from among nine hand gestures performed by a volunteer placed in the LoS of the Wi-Fi devices. The proposed system achieved an average accuracy of 90.4% among ten volunteers. Similarly, in [77], each volunteer placed his hand in the LoS of Wi-Fi devices and performed up to six hand gestures, e.g., moving the hand to the right or the left, achieving a cross-validation accuracy of 98%. In [76], authors work with the identification of four hand gestures, which, despite being fewer than those presented in the works mentioned above, explored scenarios where the volunteer was not located in the LoS of Wi-Fi. They proved that even when the volunteer is in an NLoS scenario, the developed system can achieve an average accuracy of 96%. In [89], authors presented a mechanism to reconstruct both hands' movement trajectories and identify which hand gesture is being performed out of nine possible ones using an SVM with an accuracy above 96%.

For identifying even more fine movements, authors in [71] defined finger gesture patterns for remote control functions for further identification, obtaining an accuracy of 81% using a neural network. This work also explored identifying the number of syllables from words of a sentence based on chin movements, achieving an accuracy of 92.8% by using a peak finding algorithm and introducing a virtual multipath to enhance sensing performance. Meanwhile, in [34], authors aimed to identify six facial expressions: happiness, fear, surprise, happily surprised, angrily surprised, and fearfully surprised. They used a tree-based machine learning method and collected data from 20 volunteers, achieving a cross-validation accuracy of 94.8%.

Gesture recognition technology also has practical applications; Wikey [41] aims to detect a computer keyboard keystroke and recognize which key was pressed. Authors extended the functioning of Wikey to recognize complete words from sentences with an accuracy above 85%. Moreover, the WiMorse system [72] identifies letters according to their Morse code representation, forming Dots and Dashes with specific finger movements with an accuracy of 96.6%. In addition,

Table 5
Gesture recognition applications.

Reference	Activities	Collecting tool	Communication hardware	Performance
[10]	Sign language	Atheros CSI Tool	Tx-2 OMNI antennas, Rx-3 OMNI antennas	95.8% accuracy.
[89]	1 hand and 2 hands gestures	Linux 802.11n CSI Tool	Tx-1 OMNI antenna, Rx-2 OMNI antennas	Accuracies > 96%.
[30]	WiDar 3.0 dataset [148]	Linux 802.11n CSI Tool	Tx-1 OMNI antenna, Rx-3 OMNI antennas	Accuracies ≥ 81%.
[76]	4 different hand gestures	Linux 802.11n CSI Tool	Tx and Rx-3 OMNI antennas	96% accuracy.
[77]	6 hand gestures	Atheros CSI Tool	Tx- 1 OMNI antenna, Rx-3 OMNI antennas	98% cross-validation accuracy.
[84]	WiDar 3.0 dataset [148]	Linux 802.11n CSI Tool	Tx-1 OMNI antenna, Rx-3 OMNI antennas	86.16% accuracy.
[34]	6 different facial expressions	Linux 802.11n CSI Tool	Tx-1 directional and 2 OMNI antennas, Rx-3 OMNI antennas	94.8% cross-validation accuracy.
[35]	12 different hand and finger gestures	Linux 802.11n CSI Tool	Tx-1 OMNI antenna, Rx-3 OMNI antennas	95% cross-validation accuracy.
[39]	Computer-related gestures	Linux 802.11n CSI Tool	Tx-1 OMNI antenna, Rx-3 OMNI antennas	77% accuracy.
[40]	9 finger gestures	Linux 802.11n CSI Tool	Tx-1 OMNI antenna, Rx-3 OMNI antennas	90.4% accuracy.
[41]	Keystrokes	Linux 802.11n CSI Tool	Tx-2 antennas, Rx-3 antennas, type not specified	97.5% accuracy for keystroke detection; 96.4% for keystroke recognition.
[69]	Physical therapy gestures	ESP32 CSI Toolkit	Single onboard antenna, up to 3 ESP32 as Rx	Accuracies ≥ 85.21%.
[71]	8 different finger gestures and chin movement detection	WARP Platform	Tx and Rx- 1 OMNI antenna	81% accuracy for finger gestures; 92.8% accuracy for chin movement counting.
[72]	Finger movements for morse letter recognition	Linux 802.11n CSI Tool	Tx-3 OMNI antennas, Rx-2 OMNI antennas	96.6% accuracy.
[73]	Finger tracking and digit recognition	Linux 802.11n CSI Tool	Tx-1 OMNI antenna, Rx-3 OMNI antennas	Median error of 1.27 cm for finger tracking; 90% accuracy for digit recognition.
[108]	Finger tracking for letter recognition	Linux 802.11n CSI Tool	Tx-2 OMNI antennas, Rx-3 OMNI antennas	74.84% accuracy.
[118]	WiDar 3.0 dataset [148]	Linux 802.11n CSI Tool	Tx-1 OMNI antenna, Rx-3 OMNI antennas	93.71% cross-validation accuracy.

WiMorse presents a mechanism to obtain a similar CSI waveform, despite the place where movements are performed, as they notice that waveforms could have different behaviors depending on where the actions were performed. In [73,108], authors used CSI for finger tracking to recognize digits and letters written in the air. As mentioned, hand gesture recognition can be used to recognize sign language, as it has well-defined gestures to represent letters or words. Seizing this, in [10], CSI samples were collected from 5 volunteers performing at most 12 sign language gestures, with an accuracy of 95.8%.

The use of Deep Learning for gesture recognition has also been explored, with works that used CNNS, as in [39], where they used a heat map image constructed from CSI as input to identify what a computer user was performing based on his keyboard and mouse movements with an average accuracy of 77%. Furthermore, in [35], authors reported a cross-validation accuracy of 95% for identifying 12 hand and finger gestures using a CNN with transfer learning. In [69], a work that also did activity recognition used a Dense Neural Network for gesture recognition during therapy, specifically for finger and wrist movements. This work used ESP32 microcontrollers for collecting CSI and obtained an accuracy of 85.21% and 97.13% for finger and wrist gesture recognition, respectively. Recent works [30,84,118] have explored the use of Attention Modules and Transformers for CNN to boost the performance of gesture recognition as these models have increased in popularity in recent years for Natural Language Processing. By working with the WiDar dataset [148], the models with Attention Modules and Transformers outperformed state-of-the-art architectures, proving that these new architectures can also be implemented in Wi-Fi sensing systems.

The performance and gestures detected in each presented work are summarized in Table 5.

6.3. Vital signs monitoring

Vital Signs Monitoring systems using Wi-Fi technology aim to obtain physiological data, such as breathing and heart rate, to identify the current status of a person, usually in a rest position so other movements do not create perturbations on CSI data, as they could be of a higher degree of motion compared to chest displacements occasioned by breathing or heartbeat.

As will be seen next, breathing rate can be found as the most monitored vital sign in Wi-Fi sensing systems, which focus on estimating its value or identifying breathing patterns.

6.3.1. Vital signs monitoring related work

One of the first works that explored this field was [58], where authors proposed a theory of how breathing depth, location of the person, and their orientation can affect breathing detectability, as all these parameters influence breathing rate data acquisition from CSI. To verify this theory, authors in [46] explored how the distance between transceivers affects the performance of a breathing pattern classification system in an anechoic chamber. Authors artificially added path loss to simulate distance and found that the accuracy drops from 100% to 85.02% when the distance increases from 2.3 to 72.76 m.

Frequency analysis using the FFT is commonly employed for breathing rate estimation due to the ease of implementation and the concise results obtained, as can be seen in [56], where FFT was applied to perform a frequency analysis of the processed CSI by filters and estimate breathing rate from the frequency domain in a scenario in which the person was in a bed situation, managing to identify the sleep posture with an accuracy higher than 85%. In addition to the FFT, in [71], they introduced a virtual multipath to improve sensing capabilities, thus achieving a breathing rate accuracy of 98.8%. Wiphone [92] is a system that also uses FFT for spectrum-based breathing rate estimation. However, unlike computers with the Intel 5300 NIC commonly used for Wi-Fi sensing, they use the CSI captured with a smartphone to achieve sensing. As a result, they found that breathing rate monitoring can be achieved using smartphones in NLoS scenarios with an estimation error of 0.31 breaths per minute. Similarly, in [68], they use smartphones as CSI collection devices and a voting algorithm that takes as reference the frequency with the highest magnitude of five subcarriers, resulting in an estimation error of 0.34 breaths per minute. Besides, an additional alternative to smartphones and computers is shown in [94] where they used ESP32 microcontrollers and the Wi-ESP tool [149] to collect CSI and subsequently perform breathing rate estimation from a spectrum density analysis (PSD), resulting in an accuracy of 99.6%. Similarly, in [57], authors used ESP32 to collect CSI and compare the performance for breathing rate monitoring between a Wi-Fi sensing approach and a respiration belt to validate Wi-Fi CSI from ESP32 for sensing, obtaining that about 95% of differences range between −0.27 and 0.21 breaths per minute with an RMSE of 1.04.

The FFT-based approach has the disadvantage that the frequency resolution directly depends on the FFT window size, complicating its implementation in real-time systems. Because of this, other authors have resorted to employing peak detection algorithms to achieve breathing rate estimation. For example, in [51], authors used a peak detection algorithm in conjunction with a method to eliminate multipath reflections with a high delay based on the Power Delay Profile of CSI since a multipath with a high delay is unlikely to present relevant information for indoor sensing. In [66], the performance of a breathing rate monitoring system was analyzed in a through-the-wall scenario with a maximum error of 1.75 breaths per minute. In contrast, in the other three LoS scenarios, a maximum median error of 0.29 breaths per minute was obtained. In [59], the breathing rate is estimated based on the peak-to-peak interval of CSI data processed with an algorithm for the elimination of false peaks and with a Doppler shift-based breathing model, obtaining with this approach a maximum estimation error of 0.7 breaths per minute. A method for subcarrier selection based on relevant breathing rate information was proposed in [47]. This selection method was based on the relative difference between the two highest frequency components; the higher the difference, the more breathing rate information the subcarrier has. With this approach, 80% of estimation errors obtained were below 0.38 breaths per minute.

Machine learning and deep learning algorithms have also been implemented in breathing rate monitoring systems. For example, in [90], they use an SVM first to detect the presence of a person in a room and then estimate his breathing rate with a Root-MUSIC algorithm and cluster analysis for scenarios with more than one person, achieving an accuracy of 98.65% for breathing rate estimation for up to 9 people in a LoS scenario. In [70], they also explore breathing rate estimation of multiple persons using the K-Means clustering algorithm and segment matching, obtaining mean absolute breathing rate errors of 0.21, 0.42, and 0.73 breaths per minute in scenarios with two, three, and four persons, respectively. In [82], they make use of a neural network that has as inputs features extracted from CSI, such as phase difference between antennas, mean, variance, range, and interquartile moment to associate the CSI extracted breathing signal with a normal breathing pattern, apnea state or no breathing with an accuracy of 96.12%, 98.85%, and 99.33% respectively.

In addition to breathing rate monitoring, some works have explored heart rate monitoring by estimation or pattern identification, which is a significant challenge because chest displacement caused by a heartbeat is considerably smaller than displacement caused by breathing. In [7], they use a peak detection algorithm for breathing rate estimation and determine the heart rate through Power Spectral Density analysis, obtaining estimation errors of 0.4 breaths per minute and 90% of estimations with an error below 4 beats per minute. In [52], they perform pattern matching of breathing and heart rate patterns using Dynamic Time Warping, an algorithm that results in a measure of similarity between two signals. This approach resulted in an accuracy of 94% and 90% for breathing and heart rate pattern identification, respectively. Similarly, in [64], authors applied signal decomposition techniques to extract heart rate information to calculate the difference between two consecutive heartbeats for measuring heart rate variability. They obtained an average RMSE of 143.9 with this approach and concluded that the performance could be improved by increasing the transmission power using directional antennas. This statement has been proved in [8], where directional antennas were used to improve heart rate monitoring; with the help of frequency analysis with FFT for heart rate estimation, they observed that from having an error of 4.82 beats per minute with omnidirectional antennas, which are commonly used for Wi-Fi sensing, when using directional antennas, the error is reduced to 1.19 beats per minute.

The performance of each presented work involving Vital Signs Monitoring is summarized in Table 6.

6.4. Indoor localization

Indoor Wi-Fi localization systems are designed to detect a person's location inside a room without the need for the person to carry a device with positioning services, like a smartphone.

Indoor localization can be classified into two types of applications: fingerprint-based or subspace-based. Most Wi-Fi CSI-based indoor localization systems are fingerprint-based, which involves taking numerous CSI samples from each possible location where a person can be found. These samples are then used to classify new samples based on fingerprints. On the other hand, subspace-based applications determine the person's location based on signal propagation features that can be estimated from CSI.

6.4.1. Indoor localization related work

As mentioned above, most of the presented works involving Wi-Fi Indoor Localization systems are fingerprint-based and usually rely on machine learning techniques for classification and regression. Subspace-based indoor localization does not require an offline phase where a model is trained. An example of a subspace-based indoor localization system is [88], where authors proposed a Dynamic-MUSIC method to detect reflection paths that capture the movement of a person and his position is determined by comparing the estimated angle of arrival from multiple receivers with angles previously registered for different positions in the room. The authors obtained a median error of 41 cm using four receivers with this approach. In [91], a 2-dimensional multiple packets-based matrix pencil (2D M-MP) was proposed to estimate the angle of arrival and time of flight by accumulating multiple CSI frames to improve its estimation and allow real-time localization by reducing execution time if compared to other estimation algorithms such as MUSIC. The results show that 2D M-MP presents an execution time of 0.074 s with a localization error of 0.42 meters by evaluating the angle of arrival and using triangulation for achieving localization, while the MUSIC algorithm takes up to 5.367 s with an error of 0.76 m. Later, the same authors proposed a 3-D beamspace matrix pencil algorithm [86] also to estimate the angle of arrival, time of flight, and Doppler frequency shift and a phase detection and compensation algorithm to ensure the stability of phase difference.

Table 6
Vital signs monitoring applications.

Reference	Vital signs	Collecting tool	Communication hardware	Performance
[7]	Breathing and heart rate and sleep postures	Linux 802.11n CSI Tool	Not specified	Breathing rate errors < 0.4 bpm; 98% accuracy for posture identification; heart rate errors < 4 beats.
[8]	Breathing and heart rate	Linux 802.11n CSI Tool	Tx with directional antenna	Median estimation errors of 0.25 breaths per minute and of 1.19 beats per minute.
[51]	Breathing rate	Linux 802.11n CSI Tool	Tx and Rx-3 OMNI antennas	Accuracies ≥ 90%.
[90]	Breathing rate	Commodity Wi-Fi devices	Tx and Rx-3 OMNI antennas	98.65% multi-person breathing accuracy.
[66]	Breathing rate	Linux 802.11n CSI Tool	Tx and Rx-3 OMNI antennas	Median errors of 0.25 bpm, 0.25 bpm and 0.29bpm for three different scenarios.
[82]	Breathing pattern	Linux 802.11n CSI Tool	Tx-1 OMNI antenna, Rx-3 OMNI antennas	Accuracies ≥ 96.12%.
[52]	Breathing and heart pattern	Linux 802.11n CSI Tool	Not specified	Breathing pattern identification accuracy of 94% and 90% accuracy for heart pattern identification.
[70]	Breathing rate	Linux 802.11n CSI Tool	Tx and Rx- 3 OMNI antennas	Breathing rate error of 0.73 bpm in a 4 person scenario.
[46]	Breathing pattern	Atheros CSI Tool	Tx-2 OMNI antennas, Rx-3 OMNI antennas	99.97% cross-validation accuracy.
[47]	Breathing rate and sleep postures	Linux 802.11n CSI Tool	Tx-1 OMNI antenna, Rx-3 OMNI antennas	Estimation errors < 0.38; 94.59% accuracy for posture identification.
[68]	Breathing rate	Nexmon	Tx-4 OMNI antennas, Rx-smartphone	Mean detection error of 0.34 bpm.
[56]	Breathing rate and sleep postures	not specified	2 Tx and 2 Rx	Breathing rate and posture identification accuracy > 85%.
[57]	Breathing rate	ESP32 CSI Toolkit	Single onboard antenna	RMSE of 1.04 bpm.
[59]	Breathing rate	Linux 802.11n CSI Tool	Tx and Rx-1 OMNI antenna	Breathing rate errors ≤ 0.7 bpm.
[64]	Heart rate variability	Linux 802.11n CSI Tool	Tx-1 OMNI antenna, Rx-3 OMNI antennas	RMSE of 143.9 ms.
[71]	Breathing rate	SDR-WARP Platform	Tx and Rx-1 OMNI antenna	98.8% accuracy.
[92]	Breathing rate	Nexmon	Not specified	Breathing rate error of 0.31 breaths per minute (bpm).
[94]	Breathing rate	Wi-ESP	1 ESP as Tx, 1 ESP as Tx; experiments done with onboard antenna, OMNI antennas, and directional antennas.	99.6% accuracy.

This proposal reduces execution time and reduces the median error for indoor localization from 0.48 meters with M-MP to 0.43 m.

In [123], they delimited 64 reference points in an indoor scenario and obtained 120,000 CSI samples at each point. These samples were converted to images used to train a CNN responsible for locating a person in one of those 64 points with a mean estimation error of 1.36 m, considering that the scenario had dimensions of 16.3 meters by 17.3 m. ResLoc [80] is a system that builds images from the collected CSI, as well as a CSI tensor obtained from the CSI amplitude and phase information, to serve as input to a deep learning model that at most presented a distance error of 2.46 meters and where 30% of the samples used to evaluate the model presented an error below 0.3 m. Continuing with deep learning, in [78], they used a Variational Deep Learning Network model to determine the position of a person through regression, having trained the model with a total of 113 reference points and testing it with 22 test points which were not in the reference points, obtaining as a result that their model is capable of estimating the location of a person with an accuracy of 1.28 m. Similarly, in [121], they used a deep learning network for regression, achieving errors of 1.08 and 1.50 m, respectively, in two different scenarios. In [122], they use a Bayes adaptive Kalman filter to improve the classification performance of a CNN by up to 22% in a real indoor scenario. This CNN takes as input images constructed from the combination of CSI amplitude variations of subcarriers.

Contrary to the previously mentioned works that use deep learning models, authors in [111] resorted to a more straightforward machine learning method. They used Random Forest to locate a person from 25 possible positions with an error of 0. 17 m. Similarly, in [109], they used Bayesian methods to estimate the location of a person by dividing four different scenarios into multiple cells of the same size and tracking the person through them, achieving an accuracy over 90% for cell identification and a mean absolute error of 0.63 m. In [112], they experimented with a Naive Bayes Classifier to determine a person's location in two everyday scenarios, the first with 19 reference points. In contrast, the second scenario had a total of 30 reference points, obtaining an accuracy above 90% in both scenarios. This work also considers two additional scenarios, a corridor with people passing through and a room connected to an outside balcony, obtaining an accuracy of 66.7% and 94.7% in each, respectively. On the other hand, authors in [113] used a neural network to estimate the location of a person in an indoor scenario in conjunction with an adaptive genetic algorithm to avoid the convergence of the neural network to a local optimum and using smartphones as CSI collection devices, obtaining as a result that the developed system presents errors below 4 meters in 90.47% of the experimented cases.

Table 7
Indoor localization applications.

Reference	Approach	Collecting tool	Communication hardware	Performance
[88]	Subspace-based	Linux 802.11n CSI Tool	2 Tx, antenna type and number not specified, 4 Rx-3 antennas, type not specified	Median error of 41 cm.
[78]	Fingerprint-based regression	Linux 802.11n CSI Tool	Tx-1 OMNI antenna, 16 Rx-3 OMNI antennas	Localization accuracy of 1.28 m in a complex environment.
[80]	Fingerprint-based multiclass classification	Linux 802.11n CSI Tool	Tx-1 OMNI antenna, Rx-3 OMNI antennas	Maximum distance error of 2.46 m.
[86]	Subspace-based	Nexmon	Tx-1 OMNI antenna, Rx-3 OMNI antennas	Median errors of 0.42 and 0.55 m in two different scenarios.
[91]	Subspace-based	Nexmon	Tx-1 OMNI antenna, Rx-4 OMNI antennas	Localization error of 0.42 m.
[109]	Fingerprint-based multiclass classification	Linux 802.11n CSI Tool	Not specified	Median distance error below 0.8 m.
[111]	Fingerprint-based multiclass classification	Linux 802.11n CSI Tool	4 Tx-1 OMNI antenna, Rx-1 OMNI antenna	Accuracy of 93.12% in an office environment.
[112]	Fingerprint-based multiclass classification	Linux 802.11n CSI Tool	Tx-2 OMNI antennas, Rx-3 OMNI antennas	Mean accuracy of 86% for four different scenarios.
[113]	Fingerprint-based regression	Nexmon	Cellphone as Rx	Confidence probability within 4 m is 90.47%.
[121]	Fingerprint-based regression	Linux 802.11n CSI Tool	Tx-2 OMNI antennas, Rx-3 OMNI antennas	Mean distance error of 1.08 m and 1.50 m in two scenarios.
[122]	Fingerprint-based multiclass classification	Linux 802.11n CSI Tool	Tx-3 OMNI antennas, Rx-3 OMNI antennas	Mean distance error of 0.46 and 1.11 m in LoS and NLoS scenarios.
[123]	Fingerprint-based multiclass classification	Linux 802.11n CSI Tool	Not specified	Mean estimation error of 1.36 m and standard deviation of 0.9 m.
[145]	Model-based estimation	hostapd	11 Tx, 7 Rx, antennas not specified	Median localization accuracy of 0.5 m.

An exception to subspace-based and fingerprint-based indoor localization systems is presented in [145], where a model-based approach is proposed. This approach uses a genetic algorithm to solve equations from a power fading model to achieve indoor localization, obtaining that in a LoS scenario, the model presents a median error of 0.5 m. In contrast, in an NLoS scenario, the median error grows to 1.1 m.

It is important to note that these works usually report an estimation error despite using classification models. This is because it is more understandable for the reader to interpret a location error in meters than performance metrics according to a reference point. However, it could lead to misunderstandings when comparing the performance of different systems, as the error will depend on the distance separation between points.

Table 7 summarizes the works discussed previously for Indoor Localization.

6.5. Crowd counting

Crowd counting applications determine the number of people present in a particular area. It can be used in multiple applications, for example, to identify areas of interest in a tourist site or the category of products in which buyers are most interested in a store or square; it can be used to address security problems by determining the number of people trapped in a building due to an accident or in home automation to perform intelligent control of the ventilation of a room or lighting based on the number of people.

6.5.1. Crowd counting related work

Two main approaches can be observed for crowd counting. The first approach consists of classification, where CSI fingerprints for different numbers of persons in the room are collected and used to train machine learning models or to measure the similarity between labeled signals. For example, in [117], they developed the WiCount system using a neural network to determine the number of people up to a maximum of five in a laboratory with two different datasets. In the first dataset, volunteers remained static, while in the other, they were free to move, obtaining an accuracy of 82.3%. In [119], authors collected CSI fingerprints with one and nine people in the scenario. They performed the classification task using deep learning with an accuracy of 88%, observing that with a maximum of seven people, up to 90% of the network responses had an error less than or equal to two.

By using deep learning, the authors in [79] use the CSI phase information to estimate the number of people and determine their location using the MUSIC algorithm as a basis for the visualization of the distribution of people in the scenario with accuracy and recall above 97% for crowd counting. As an extension of activity recognition, authors in [5] explored using an LSTM for crowd counting with two different datasets. The first dataset contains information about one to three people doing activities such as sitting, standing up, and walking in the same room. It also counts the number of people based on the activities occurring in the room. In contrast, the second one is not related to any activity and contains four possible classes, from empty to three people in the room, obtaining an overall accuracy of 99.72% for the activity dataset for crowd counting and 97.40% for the second dataset. Wifree [96] is another crowd counting system with a classification approach. It can identify up to seven people in an indoor scenario. In Wifree, they used transfer kernel learning because samples collected with the same number of people at different moments can result in different behaviors, leading to different results. With the use of transfer learning, Wifree presents an accuracy of 92.8%, where 97% of the errors are less than one person. Also, in [55], authors evaluated the performance of a crowd counting system in a scenario where the receiver of the Wi-Fi signal was in another room separated by a wall, and by using a neural network, they obtained an average accuracy above 90%. Lastly, for classification, in [48], authors used the Probability Mass Function as an image to serve as an input to a CNN, obtaining accuracies above 82% for scenarios with zero to four people. On the contrary, in [63], authors chose not to use a learning model. Instead, they utilized Dynamic Time Warping to determine how much

Table 8
Crowd counting applications.

Reference	Approach	Collecting tool	Communication hardware	Performance
[5]	Group classification	Linux 802.11n CSI Tool	Tx-1 antenna, Rx-3 antennas, type not specified	99.72% accuracy for counting up to 3 people doing activities in a room.
[75]	Estimation	Linux 802.11n CSI Tool	Not specified	Accuracy over 81% for crowd counting in different rooms.
[55]	Group classification	Linux 802.11n CSI Tool	Tx-1 antenna, Rx-3 antennas	Accuracies of 88.76% and 91.27% in two scenarios.
[79]	Group classification	Linux 802.11n CSI Tool	Not specified	Precision of 98.2% and 97% in two scenarios.
[67]	Estimation	ESP32 CSI Toolkit	Single onboard antenna	± 2.5 counting error for up to 20 people.
[48]	Group classification	Nexmon	Not specified	Accuracies > 82% for up to 4 people.
[96]	Group classification	Atheros CSI Tool	Tx-3 OMNI antennas, Rx-3 OMNI antennas	Accuracy of 92.8% for crowd counting.
[61]	Estimation	ESP32 CSI Toolkit	Single onboard antenna	Median absolute error of 0.41 with up to 10 people.
[63]	Group classification	Linux 802.11n CSI Tool	Tx-1 OMNI antenna, Rx-3 OMNI antennas	Accuracy of 100% to 75% for one to five people.
[93]	Estimation	Not specified	Tx and Rx-3 OMNI antennas	Accuracy of 87.14%, estimation errors around 1 person.
[117]	Group classification	Not specified	Tx-2 antennas, Rx-3 antennas	Accuracy of 82.3% for up to five people.
[119]	Group classification	Linux 802.11n CSI Tool	Tx-1 antenna, Rx-2 antennas	Accuracy of 96.90% to 88.66% from one to nine people.

a filtered CSI signal resembled signals from a previously constructed database with up to five people, showing that the system presents an average accuracy of 75% in a small space.

The second approach aims to determine the number of people by estimation from CSI data, e.g., in [93], they determine the number of people based on the number of breathing signals detected by performing a spectrum analysis with an accuracy of 87.14%. Meanwhile, in [75], they extracted features such as the variance of the CSI amplitude, its range of values, and the phase difference of each subcarrier that are defined in a logistic bounded model for regression, which allows estimating the number of people with an accuracy above 89% when the model is built from samples collected in the same evaluation scenario, while in cases where different scenarios are involved, the accuracy reaches an accuracy of 83%. Continuing with regression models, in [61], they employed multiple machine learning regression models with CSI collected from ESP32 microcontrollers and even extended the system's functionality to people location in a 4-section division of a room, obtaining a mean absolute error for crowd counting of 0.41 and an accuracy of 98.1% for localization with up to 10 volunteers. Similarly, in [67], a Deep Neural Network for regression was used for counting from 0 to 20 people in steps of 5 from CSI also collected from ESP32 microcontrollers. This approach led to obtaining a counting error of *pm* 2.5 people for 76.5% of the cases.

The approach, collecting tool, communication hardware and performance obtained from each work for Crowd Counting are summarized in Table 8.

6.6. Human pose estimation

The development of Human Pose Estimation systems using CSI of a Wi-Fi signal has been explored in the last three years, but only a few works have been found because of the complexity of the task. Human Pose Estimation consists of defining a 3D skeleton that represents a person's current position and determining the position of each of their joints and limbs.

In general, Human Pose Estimation systems aim to satisfy needs in Human–Computer Interaction applications that could require knowing the current pose of the person, e.g., virtual reality applications for entertainment purposes such as Microsoft Kinect or medical training with the help of extended reality [116].

6.6.1. Human pose estimation related work

WiPose [115] is one of the first systems for estimating 3D Human Pose using commercial Wi-Fi devices. WiPose aims to reconstruct 3D human body skeletons using commercial Wi-Fi devices and deep learning models for classification, resulting in a joint localization error of 2.83 cm. In [97], they build images from CSI and use them as input for a deep learning network designed to map CSI images to human skeleton images. In addition, GoPose [116] estimates human pose and tracks free-form movements of multiple limbs based on the reflection of Wi-Fi signals. They used the bi-dimensional angle of arrival of the reflected signals to identify moving limbs and estimate the position and trajectory of each limb using multiple transmitter–receiver pairs. GoPose can track 3D human poses with an average joint localization error of 4.7 cm.

Recent approaches make use of self-attention and multi-head attention modules for enhancing pose estimation, such as in [83,124], which evaluated the trained model using the Percentage of Correct Key Points (PCK) with a threshold of 50%, obtaining values of 96.80% and 88.74%, respectively. Additionally, in [83], authors proposed an Attention-Based subcarrier selection model to pay more attention to feature-rich subcarriers, being the first seen work that applies deep learning for subcarrier selection.

Table 9 summarizes the presented works related to Human Pose Estimation.

6.7. Gait analysis

Wi-Fi Gait Analysis sensing systems make use of CSI to find values associated with gait, such as the number of steps, pace, or the number of steps for diverse purposes, e.g., monitoring athletes' warm-up exercises [60] or the state of patients with Parkinson's [102], and as an auxiliary tool for gait therapies. Moreover, gait analysis can support people's identification, as shown in Wi-Fi systems for People Identification. Table 10 summarizes the works selected for this section.

Table 9
Human pose estimation applications.

Reference	Collecting tool	Communication hardware	Performance
[83]	Linux 802.11n CSI Tool	Tx-3 OMNI antennas, Rx-3 OMNI antennas	88.74% of correct keypoints for PCK 50.
[97]	Linux 802.11n CSI Tool	Tx-1 OMNI antenna, 2 Rx-3 OMNI antennas	Over 25% of captured human pose images matched the ground-truth skeleton strictly.
[115]	Linux 802.11n CSI Tool	Tx- 1 OMNI antenna, 3 Rx-3 OMNI antennas	It can localize each joint on the human skeleton with an average error of 2.83 cm.
[116]	Linux 802.11n CSI Tool	Tx-3 OMNI antennas, 4 Rx-3 OMNI antennas	Median joint estimation error of 4.3 cm. The average joint localization error ranges from 3 to 8.4 cm.
[124]	Atheros CSI Tool	Tx-1 OMNI antenna, Rx-3 OMNI antennas	96.8% of correct keypoints for PCK 50.

Table 10
Gait analysis applications.

Reference	Gait parameter	Collecting tool	Communication hardware	Performance
[43]	Cadence, walking distance, step length, and walking direction	Linux 802.11n CSI Tool	2 Tx and 2 Rx, antenna types or number not specified	Estimation error of 0.02-0.16 m for step length, 0.01-0.16 Hz for cadence, and less than 8.84 degrees for walking direction.
[60]	Number of steps	Linux 802.11n CSI Tool	Tx-1 antenna, Rx- 3 antennas (type not specified)	Step estimation accuracy of 93.18%, 91.73%, 90.25%, 88.44%, and 81.4% for one to five runners.
[102]	Freeze of gait detection, as well as walking slow, voluntary stop, walking fast, sit and stand up classification.	Linux 802.11n CSI Tool	Tx and Rx-1 OMNI antenna	By doing data fusion with radar signals, mean accuracy of 98.1%.
[143]	Walking distance	Linux 802.11n CSI Tool	Tx-2 OMNI antennas, Rx-3 OMNI antennas	Mean absolute percentage error of 4.85%.

6.7.1. Gait analysis related work

WiSpeed [143], which was presented as a system able to detect falls, also estimates pace and stride length with a pace mean absolute percentage error of 4.85% and establishes that the number of steps, as well as the stride length, can be estimated from the found pace. However, they do not present quantitative results of these last two parameters. Besides, in [43], authors presented quantitative results for stride length, pace, distance walked, and direction. They found that the developed system presents an estimation error for step length between 0.02 and 0.16 meters for a pace between 0.01 and 0.16 Hz, translating to an error between 0.6 and 9.6 steps per minute. While walking direction, they found that their system presents errors below 8.84 degrees as long as the person walks straight. In [60], authors used a peak detection algorithm and a series of filters to determine the number of steps from up to five people, isolating the corresponding signal from each person with the help of Canonical Polyadic Decomposition. With this proposal, they obtained step estimation accuracies of 93.18% and 81.4% for one and five people, respectively. Finally, in [102], authors aimed to identify the freeze of gait, whether the person had stopped voluntarily, and whether the person was walking fast or slow. This is to monitor people with Parkinson's through the combination of scalograms obtained from Wi-Fi CSI and spectrograms acquired by a radar sensor. Both serve as inputs to a deep learning model that gives an average accuracy between the abovementioned events and activities of 98.1%.

6.8. Presence detection

Presence Detection, also known as Occupancy Detection, as its name suggests, detects the presence of people inside a room and can be implemented for several purposes, e.g., security, by detecting the presence of a person in a place where he/she should not be. In home automation, to turn on and off lights depending on whether the room is occupied or as a first step for other Wi-Fi sensing applications to start once a person is detected.

6.8.1. Presence detection related work

As with Indoor Localization and Crowd Counting, systems for presence detection can be based on obtaining CSI fingerprints while a room is empty and occupied, such is the case of [103], where they took 2000 CSI samples from a room with human presence and being empty. Then, they applied PCA to reduce the computational complexity of CSI fingerprints used to train an SVM, resulting in a human presence detection accuracy higher than 97%. In [142], authors use Euclidean distance to measure the similarity between CSI fingerprints previously labeled in an offline phase and CSI fingerprints collected in an online phase, even identifying whether the person in the room is static or moving, with a detection rate above 90%. Authors in [99] developed a platform that integrates Wi-Fi devices, a server in the cloud, and a user program to detect the presence of people, where the server is responsible for performing machine learning computations, resulting in an accuracy of 96.8%. In [49], machine learning models such as K-Nearest Neighbors, SVM, Decision Trees, and Naive Bayes were tested to find which is adequate for presence detection. The highest cross-validation accuracy was obtained with the SVM, with 92% accuracy, using the max and mean value as input, the number of abrupt changes in the time series, and the standard deviation. An SVM model was also used by authors in [62], where they use the similarity measurement obtained from Dynamic Time Warping as a feature with 233 other features, obtaining an accuracy of 99.21%.

In addition to traditional machine learning algorithms, deep learning has also been implemented for presence detection, as in [81], where deep learning networks are used by taking as inputs two different images constructed from the Discrete Fourier Transform of the CSI amplitude and phase data, thus obtaining an accuracy of 95.55%. Similarly, in [110], authors focused on the detection of infant presence in the back of a vehicle, differentiating it from a pet or an object based on CSI Radio Images, which is nothing more than a graphical representation of the CSI matrix formed by amplitude and phase values of each subcarrier.

Unlike fingerprint-based applications, in WiFree [96] authors used a threshold-based method to identify whether CSI data contain information of an occupied or an empty space by using an index to measure

Table 11
Presence Detection.

Reference	Collecting tool	Communication hardware	Performance
[81]	Atheros CSI Tool	Tx-3 antennas, Rx-3 antennas	Presence detection performance of 95.55%.
[49]	Linux 802.11n CSI Tool	Tx-2 OMNI antennas, Rx-3 OMNI antennas	92% cross-validation accuracy.
[96]	Atheros CSI Tool	Tx-3 OMNI antennas, Rx-3 OMNI antennas	Presence detection accuracy of 99.1%.
[99]	Linux 802.11n CSI Tool	Tx-1 antenna, Rx-3 antennas	Presence detection accuracy of 96.8%.
[62]	Nexmon	Not specified	Accuracies > 99%.
[103]	Linux 802.11n CSI Tool	Tx-2 antennas, Rx-3 antennas	Presence detection precision over 97%.
[110]	Linux 802.11n CSI Tool	Tx-3 OMNI antennas, Rx-3 OMNI antennas	Presence detection accuracy above 95%.
[142]	Linux 802.11n CSI Tool	Tx-1 antenna, Rx-3 antennas	Presence detection accuracy above 96%.
[144]	Linux 802.11n CSI Tool	Commercial router as Tx, Rx-3 antennas	Presence detection accuracy above 98%.

the similarity between the amplitude curves of different subcarriers, establishing that, if the index exceeded the threshold, the room was occupied. In [144], authors calculated a motion indicator based on the correlation of CSI time and frequency domain data since they found that when there is no one in the room, the cross-correlation between CSI samples is considerably higher if compared to when a person is present. Hence, the room is occupied if the motion indicator is below a threshold. This approach led them to achieve an accuracy higher than 98%.

The performance of presence detection works previously discussed is shown in Table 11.

6.9. People identification

People Identification systems attempt to identify a specific person from among a group of n people based on the Wi-Fi signal variations caused by that specific person. It can be implemented for different purposes, e.g., intrusion detection, thus assuring that only authorized personnel can access a particular area or resource. On the other hand, in home automation, people identification can be used to adjust a room condition based on the person's preference. The maximum number of people and the performance obtained for each work that will be discussed in this section is shown in Table 12.

6.9.1. People identification related work

People identification can be performed by extracting features from CSI data that characterize a particular person. For example, in [31], authors implemented k-NN that uses Dynamic Time Warping as the distance metric between the CSI waveform captured when the person passes through the LoS of the Wi-Fi devices and labeled CSI waveforms, achieving an accuracy of 94.5% to 75% when increasing the size of the group from two to nine people. A term that can be found in People Identification literature is *Radio Biometrics*; explored in [85], by using a time-reversal technique, authors performed people identification in a through-the-wall scenario, achieving an accuracy of 98.78% with a group of 11 people. Radio biometrics is defined as the wireless signal altered by the presence of a person that contains information about the person's identity. In [104], authors took CSI samples of up to seven different people who sat in the driver's seat of a vehicle and, by implementing a neural network in the people identification system, an accuracy of 99.13% was achieved when the group size was of two, decreasing to 53.85% with a group size of seven. This led the authors to conclude that the performance decreases as the group size increases because radio biometrics are more likely to be similar between volunteers. In [98], to enhance data collection from CSI, the authors placed a metal plate in front of the transmitter to generate multipaths following a model based on Rician fading. With this addition and a deep learning network, they achieved an accuracy of 94.3% for recognizing between a spoofer and a legitimate user (binary classification). Similarly, in [42] people identification between legitimate users and spoofers utilizing an SVM, with the addition to identifying which legitimate user is achieved by extracting a feature vector from a combination of gestures, thus obtaining an average accuracy of 92.9% for the identification of up to ten legitimate users. In contrast, in 7.3% of cases, a spoofer was mistaken for a legitimate user.

Another approach for achieving People Identification is through gait analysis because when walking, a person could have characteristic body movement patterns that can be used to distinguish a person among a group of people. As in [53], where authors implemented high delay multipath removal as a filtering technique based on the PDP and, by using a tree-based machine learning classifier which had as inputs extracted features from gait patterns, they achieved accuracies from 92% to 80% when the group size varies from two to six people respectively. In [45], an SVM extracted and used gait features from the time and frequency domain, achieving an accuracy of 90.9% for a group size of eight. In addition, the authors claimed that the developed system can identify if a person is a stranger or if he belongs to the registered group; however, the system receives prior training with data from possible strangers, so they are not strangers to the system at all. Similar to the previous ones, in [105], authors made a system that identifies people based on the characteristics of the person's gait, with the difference that in this work, they generate a spectrogram to observe how the movement of different body parts is present at different frequencies. Then, 10901 features are extracted from the spectrogram and serve as the input for an SVM, presenting an accuracy of 92.83% to 78.28% when the group size varies from three to six people. GaitID [11] is another system that extracts gait features to perform people identification in which the CSI Gait-body coordinate velocity profile is proposed. This aims to represent the velocities for different body parts during gait and whose characteristics serve as input to a deep learning network, thus achieving the identification of 11 people with an accuracy of 76.2%, 99% for two people, and 93.2% for five people. The GaitID system also uses transfer learning to speed up model training when a new user is added to the identification system.

Breathing and heart rate patterns extracted from CSI data can also be used to identify people. This has been shown in [54], where chest displacements caused by cardiopulmonary activity are taken as reference for identifying from a group size of two to five persons with accuracies from 84% to 65% respectively. Likewise, features from gait and breathing patterns were extracted in [44] and used as inputs to a deep learning network that led to an accuracy of 98.33% with a group size of 15 people.

7. Wi-fi remote sensing challenges

7.1. CSI availability

As mentioned in Section 3, CSI is physical layer information not provided by Wi-Fi devices unless changes are made to their firmware, considerably reducing the number of devices that can be used for CSI data collection to a few of the market, such as Intel 5300 NICs and some Atheros chipsets, which work with the outdated 802.11n communication standard. However, recent works have proposed using ESP32s as collection devices for CSI. These devices are a low-cost and scalable alternative to the limited number of devices that can be used for CSI data collection but still work under the 802.11n Wi-Fi standard.

Table 12
People identification.

Reference	Max people No.	Collecting tool	Communication hardware	Performance
[11]	11	Linux 802.11n CSI Tool	1 Tx, 6 Rx	Accuracy of 76.2% for identificating 11 people.
[31]	9	Linux 802.11n CSI Tool	Tx-2 antennas, Rx-3 antennas	Accuracy of 94.5% to 75.5% while varying the number of people.
[42]	10	Linux 802.11n CSI Tool	Tx-2 OMNI antennas, 2 Rx-3 OMNI antennas	Mean accuracy of 92.9%.
[44]	15	Linux 802.11n CSI Tool	Tx-3 OMNI antennas, Rx-1 OMNI antenna	Accuracy in a non-interference environment of 98.33%.
[45]	8	Linux 802.11n CSI Tool	Tx-1 OMNI antennas, Rx-3 OMNI antennas	Accuracy from 98.7% to 90.9% while varying the number of people.
[53]	6	Linux 802.11n CSI Tool	Tx-3 OMNI antennas, Rx-3 Omni antennas	Accuracy of 92% to 80% while varying the number of people.
[54]	5	Linux 802.11n CSI Tool	Tx-1 OMNI antenna, Rx-2 OMNI antennas	Accuracy of 84% to 65% while varying the number of people.
[98]	19 (binary classification)	Linux 802.11n CSI Tool	Tx-1 OMNI antenna, Rx-1 OMNI antenna	Accuracy of 94.3% in a real environment.
[85]	11	Not specified	Tx-3 OMNI antennas, Rx-3 OMNI antennas	Accuracy of 98.78% achieved for 11 people.
[104]	7	Not specified	Tx-2 antennas, Rx-3 antennas	Accuracy of 99.13% to 53.85% while varying the number of people.
[105]	6	Linux 802.11n CSI Tool	Tx-1 OMNI antenna, 2 Rx-3 OMNI antennas	Accuracy of 92.82% to 78.28% while varying the number of people.

Another alternative is openwifi, which uses Xilinx Zynq system-on-chip (SoC) that comes with an FPGA and ARM processor to run a SDR system with support for 802.11a/g/n Wi-Fi standards [128], or Nexmon for embedded devices [125–127], which can work with recent 802.11ac/ax Wi-Fi standards depending on the device where Nexmon is implemented.

7.2. NLoS sensing

NLoS scenarios are still a challenge to this day, as Wi-Fi sensing systems show that despite being able to achieve sensing in these scenarios, the reliability of the system response is reduced. This challenge may be addressed by considering multiple Wi-Fi devices that can be found indoors, such as IoT devices, exploiting spatial diversity. However, as mentioned before, CSI availability is still a challenge, and counting multiple Wi-Fi devices reporting CSI could lead to the next challenge.

7.3. Data density

A greater number of devices reporting CSI can be translated to a greater amount of data that needs to be processed, which is a challenge that needs to be addressed when designing real-time Wi-Fi sensing systems. Instead of preprocessing CSI by software, a solution might be to use Programmable Logic Devices, such as FPGAs, to handle the CSI preprocessing step by hardware.

7.4. Wi-Fi communications and sensing coexistence: the IEEE 802.11bf amendment

Wi-Fi 802.11n communication standard is designed for data transmission and not for sensing. Wi-Fi network performance could be affected by using a Wi-Fi device for sensing as resources are utilized to obtain CSI measurements. In addition to this, wireless signals are compensated in conventional communication standards, and this compensation might not be suitable for sensing requirements. Currently, there are efforts to develop a new standard amendment for Wi-Fi sensing called IEEE 802.11bf, which aims to address this and the previously mentioned challenges by defining a standard for the IEEE 802.11 physical layer and medium access control to enhance Wi-Fi device's sensing capabilities and to facilitate the deployment of Wi-Fi sensing systems. The main contribution of the 802.11bf amendment is the definition of the Wireless Local Area Network sensing procedure in sub-7 GHz bands and mmWave bands. This procedure has been named the Directional Multi-Gigabit (DMG) sensing procedure and is formed by a sensing initiator, which initiates the sensing; a sensing responder(s), which participates in the sensing and responds to the sensing initiator; a sensing transmitter, that sends PHY Protocol Data Units (PPDUs) used for sensing, and a sensing receiver, which performs the sensing measurements using the PPDUs [150]. It is expected that 802.11bf also introduces protected management frames for the sensing measurement report transmission to prevent adversarial attacks against the sensing service, to implement encryption so only trusted devices can retrieve data frames for CSI estimation, and to make sensing robust to interference due to shared spectrum [129].

7.5. Security concerns

This challenge arises from one of the objectives of Wi-Fi sensing and the 802.11bf standard: any network device facilitates obtaining information from the environment for any of the applications mentioned above and provides network services. This can be categorized as a potential breach of user's privacy since the sensing system does not present the limitations of, for example, surveillance cameras, which can only obtain information about what is in their line-of-sight, while Wi-Fi sensing systems may be able to sense through walls. Another scenario to consider is spoofing, in which a malicious or unauthorized user captures network-level information and information collected through Wi-Fi sensing systems, which could be translated into any of the previously mentioned applications. Protecting users and convincing them that this technology does not compromise their personal information is one of the challenges that must be addressed once commercial Wi-Fi sensing systems are developed. A rising concept for avoiding spoofing and keeping users' privacy is CSI obfuscation, which blurs CSI for unauthorized users while maintaining sensing capabilities. Some approaches for achieving this have been injecting in the channel artificial signal reflections [151], changing features of the signal with antenna switching according to a shared switching rule between authorized users [152], randomization of CSI by applying distortions to the frame with SDR [153], and adding an obfuscation layer to the openwifi project [154,155] as it allows changes to the PHY layer with Verilog Hardware Description Language (HDL).

8. Conclusions

In this work, we provided an SLR on Wi-Fi sensing with CSI, presenting an overview of what CSI is and the operational methodology of Wi-Fi sensing systems, which is composed of 4 stages: Data Collection, Data Preprocessing, Detection Algorithm, and the Human Sensing Application. We presented standard methods and techniques implemented in each step and the works that have applied them. These works were also classified and discussed according to their type of sensing application, noticing that every work presents promising results that show why Wi-Fi sensing has raised the interest of researchers worldwide. We also point out current challenges, highlighting that there are efforts to develop a new Wi-Fi standard for Wi-Fi sensing. We hope this survey can serve as a foundation for researchers starting to work with Wi-Fi sensing by providing them with directions on exploiting Wi-Fi as a sensing technology.

CRediT authorship contribution statement

Jesus A. Armenta-Garcia: Writing – review & editing, Writing – original draft, Investigation. **Felix F. Gonzalez-Navarro:** Writing – review & editing, Methodology, Investigation. **Jesus Caro-Gutierrez:** Writing – review & editing, Methodology, Investigation.

Declaration of competing interest

The authors declare that they have no known competing financial interests or personal relationships that could have appeared to influence the work reported in this paper.

Data availability

No data was used for the research described in the article.

Acknowledgments

We would like to thank CONACyT and UABC-22th Research Funding Program for their support on the development of this investigation.

References

[1] Wi-Fi Alliance, Wi-Fi alliance celebrates 25 years of innovation and impact, 2024, URL https://www.wi-fi.org/news-events/newsroom/wi-fi-alliance-celebrates-25-years-of-wi-fi-innovation-and-impact#_ftn1.

[2] G.M. Weiss, J.L. Timko, C.M. Gallagher, K. Yoneda, A.J. Schreiber, Smartwatch-based activity recognition: A machine learning approach, in: 2016 IEEE-EMBS International Conference on Biomedical and Health Informatics, BHI, 2016, pp. 426–429, http://dx.doi.org/10.1109/BHI.2016.7455925.

[3] N. Alshurafa, W. Xu, J.J. Liu, M.-C. Huang, B. Mortazavi, C.K. Roberts, M. Sarrafzadeh, Designing a robust activity recognition framework for health and exergaming using wearable sensors, IEEE J. Biomed. Health Inf. 18 (5) (2014) 1636–1646, http://dx.doi.org/10.1109/JBHI.2013.2287504.

[4] M. Javan Roshtkhari, M.D. Levine, Human activity recognition in videos using a single example, Image Vis. Comput. 31 (11) (2013) 864–876, http://dx.doi.org/10.1016/j.imavis.2013.08.005, URL https://www.sciencedirect.com/science/article/pii/S0262885613001315.

[5] N. Damodaran, E. Haruni, M. Kokhkharova, J. Schäfer, Device free human activity and fall recognition using WiFi channel state information (CSI), CCF Trans. Perv. Comput. Interact. 2 (1) (2020) 1–17, http://dx.doi.org/10.1007/s42486-020-00027-1.

[6] J. Liu, H. Liu, Y. Chen, Y. Wang, C. Wang, Wireless sensing for human activity: A survey, IEEE Commun. Surv. Tutor. 22 (3) (2020) 1629–1645, http://dx.doi.org/10.1109/COMST.2019.2934489.

[7] J. Liu, Y. Chen, Y. Wang, X. Chen, J. Cheng, J. Yang, Monitoring vital signs and postures during sleep using WiFi signals, IEEE Internet Things J. 5 (3) (2018) 2071–2084, http://dx.doi.org/10.1109/JIOT.2018.2822818.

[8] X. Wang, C. Yang, S. Mao, On CSI-based vital sign monitoring using commodity WiFi, ACM Trans. Comput. Healthc. 1 (3) (2020) http://dx.doi.org/10.1145/3377165.

[9] T. Nakamura, M. Bouazizi, K. Yamamoto, T. Ohtsuki, Wi-Fi-based fall detection using spectrogram image of channel state information, IEEE Internet Things J. 9 (18) (2022) 17220–17234, http://dx.doi.org/10.1109/JIOT.2022.3152315.

[10] Z. Hao, Y. Duan, X. Dang, Y. Liu, D. Zhang, Wi-SL: Contactless fine-grained gesture recognition uses channel state information, Sensors 20 (14) (2020) http://dx.doi.org/10.3390/s20144025, URL https://www.mdpi.com/1424-8220/20/14/4025.

[11] Y. Zhang, Y. Zheng, G. Zhang, K. Qian, C. Qian, Z. Yang, GaitID: Robust Wi-Fi based gait recognition, in: D. Yu, F. Dressler, J. Yu (Eds.), Wireless Algorithms, Systems, and Applications, Springer International Publishing, Cham, 2020, pp. 730–742.

[12] S. Shao, M. Fan, C. Yu, Y. Li, X. Xu, H. Wang, Machine learning-assisted sensing techniques for integrated communications and sensing in WLANs : Current status and future directions, Prog. Electromagn. Res. 175 (2022) 45–79, http://dx.doi.org/10.2528/pier22042903.

[13] Y. Ma, G. Zhou, S. Wang, WiFi sensing with channel state information: A survey, ACM Comput. Surv. 52 (3) (2019) http://dx.doi.org/10.1145/3310194.

[14] J.C. Soto, I. Galdino, E. Caballero, V. Ferreira, D. Muchaluat-Saade, C. Albuquerque, A survey on vital signs monitoring based on Wi-Fi CSI data, Comput. Commun. 195 (2022) 99–110, http://dx.doi.org/10.1016/j.comcom.2022.08.004, URL https://www.sciencedirect.com/science/article/pii/S0140366422003127.

[15] Z. Wang, K. Jiang, Y. Hou, W. Dou, C. Zhang, Z. Huang, Y. Guo, A survey on human behavior recognition using channel state information, IEEE Access 7 (2019) 155986–156024, http://dx.doi.org/10.1109/ACCESS.2019.2949123.

[16] M.A.A. Al-qaness, M. Abd Elaziz, S. Kim, A.A. Ewees, A.A. Abbasi, Y.A. Alhaj, A. Hawbani, Channel state information from pure communication to sense and track human motion: A survey, Sensors 19 (15) (2019) http://dx.doi.org/10.3390/s19153329, URL https://www.mdpi.com/1424-8220/19/15/3329.

[17] Y. He, Y. Chen, Y. Hu, B. Zeng, WiFi vision: Sensing, recognition, and detection with commodity MIMO-OFDM WiFi, IEEE Internet Things J. 7 (9) (2020) 8296–8317, http://dx.doi.org/10.1109/JIOT.2020.2989426.

[18] S. Tan, Y. Ren, J. Yang, Y. Chen, Commodity WiFi sensing in ten years: Status, challenges, and opportunities, IEEE Internet Things J. 9 (18) (2022) 17832–17843, http://dx.doi.org/10.1109/JIOT.2022.3164569.

[19] Y. Ge, A. Taha, S.A. Shah, K. Dashtipour, S. Zhu, J. Cooper, Q.H. Abbasi, M.A. Imran, Contactless WiFi sensing and monitoring for future healthcare - emerging trends, challenges, and opportunities, IEEE Rev. Biomed. Eng. 16 (2023) 171–191, http://dx.doi.org/10.1109/RBME.2022.3156810.

[20] S.M. Hernandez, E. Bulut, WiFi sensing on the edge: Signal processing techniques and challenges for real-world systems, IEEE Commun. Surv. Tutor. 25 (1) (2023) 46–76, http://dx.doi.org/10.1109/COMST.2022.3209144.

[21] IEEE Standard for Information Technology– Local and Metropolitan Area Networks– Specific Requirements– Part 11: Wireless LAN Medium Access Control (MAC)and Physical Layer (PHY) Specifications Amendment 5: Enhancements for Higher Throughput, IEEE Std 802.11n-2009 (Amendment to IEEE Std 802.11-2007 as Amended by IEEE Std 802.11k-2008, IEEE Std 802.11r-2008, IEEE Std 802.11y-2008, and IEEE Std 802.11w-2009), 2009, pp. 1–565, http://dx.doi.org/10.1109/IEEESTD.2009.5307322.

[22] Y. Xie, Z. Li, M. Li, Precise power delay profiling with commodity Wi-Fi, IEEE Trans. Mob. Comput. 18 (6) (2019) 1342–1355, http://dx.doi.org/10.1109/TMC.2018.2860991.

[23] E. Khorov, A. Kiryanov, A. Lyakhov, G. Bianchi, A tutorial on IEEE 802.11ax high efficiency WLANs, IEEE Commun. Surv. Tutor. 21 (1) (2019) 197–216, http://dx.doi.org/10.1109/COMST.2018.2871099.

[24] T. Paul, T. Ogunfunmi, Wireless LAN comes of age: Understanding the IEEE 802.11n amendment, IEEE Circuits Syst. Mag. 8 (1) (2008) 28–54, http://dx.doi.org/10.1109/MCAS.2008.915504.

[25] S. Zhou, L. Guo, Z. Lu, X. Wen, Z. Han, Wi-monitor: Daily activity monitoring using commodity Wi-Fi, IEEE Internet Things J. 10 (2) (2023) 1588–1604, http://dx.doi.org/10.1109/JIOT.2022.3210378.

[26] D. Halperin, W. Hu, A. Sheth, D. Wetherall, Tool release: Gathering 802.11n traces with channel state information, SIGCOMM Comput. Commun. Rev. 41 (1) (2011) 53, http://dx.doi.org/10.1145/1925861.1925870.

[27] Y. Xie, Z. Li, M. Li, Precise power delay profiling with commodity WiFi, in: Proceedings of the 21st Annual International Conference on Mobile Computing and Networking, MobiCom '15, ACM, New York, NY, USA, 2015, pp. 53–64, http://dx.doi.org/10.1145/2789168.2790124, URL http://doi.acm.org/10.1145/2789168.2790124.

[28] S.M. Hernandez, E. Bulut, Lightweight and standalone IoT based WiFi sensing for active repositioning and mobility, in: 21st International Symposium on "a World of Wireless, Mobile and Multimedia Networks" (WoWMoM), WoWMoM 2020, Cork, Ireland, 2020.

[29] Espressif, Wi-Fi driver, 2017, URL https://docs.espressif.com/projects/esp-idf/en/latest/esp32/api-guides/wifi.html.

[30] G. Tong, Y. Li, H. Zhang, N. Xiong, A fine-grained channel state information-based deep learning system for dynamic gesture recognition, Inform. Sci. 636 (2023) 118912, http://dx.doi.org/10.1016/j.ins.2023.03.137, URL https://www.sciencedirect.com/science/article/pii/S002002552300467X.

[31] T. Xin, B. Guo, Z. Wang, M. Li, Z. Yu, X. Zhou, FreeSense: Indoor human identification with Wi-Fi signals, in: 2016 IEEE Global Communications Conference, GLOBECOM, 2016, pp. 1–7, http://dx.doi.org/10.1109/GLOCOM.2016.7841847.

[32] S. Arshad, C. Feng, Y. Liu, Y. Hu, R. Yu, S. Zhou, H. Li, Wi-chase: A WiFi based human activity recognition system for sensorless environments, in: 2017 IEEE 18th International Symposium on a World of Wireless, Mobile and Multimedia Networks, WoWMoM, 2017, pp. 1–6, http://dx.doi.org/10.1109/WoWMoM.2017.7974315.

[33] X. Wu, Z. Chu, P. Yang, C. Xiang, X. Zheng, W. Huang, TW-see: Human activity recognition through the wall with commodity Wi-Fi devices, IEEE Trans. Veh. Technol. 68 (1) (2019) 306–319, http://dx.doi.org/10.1109/TVT.2018.2878754.

[34] Y. Chen, R. Ou, Z. Li, K. Wu, WiFace: Facial expression recognition using Wi-Fi signals, IEEE Trans. Mob. Comput. 21 (1) (2022) 378–391, http://dx.doi.org/10.1109/TMC.2020.3001989.

[35] Q. Bu, G. Yang, X. Ming, T. Zhang, J. Feng, J. Zhang, Deep transfer learning for gesture recognition with WiFi signals, Pers. Ubiquitous Comput. 26 (3) (2022) 543–554, http://dx.doi.org/10.1007/s00779-019-01360-8, URL https://doi.org/10.1007/s00779-019-01360-8.

[36] F. Xiao, J. Chen, X. Xie, L. Gui, L. Sun, R. Wang, SEARE: A system for exercise activity recognition and quality evaluation based on green sensing, IEEE Trans. Emerg. Top. Comput. 8 (3) (2020) 752–761, http://dx.doi.org/10.1109/TETC.2018.2790080.

[37] A. Zhu, Z. Tang, Z. Wang, Y. Zhou, S. Chen, F. Hu, Y. Li, Wi-ATCN: Attentional temporal convolutional network for human action prediction using WiFi channel state information, IEEE J. Sel. Top. Sign. Proces. 16 (4) (2022) 804–816, http://dx.doi.org/10.1109/JSTSP.2022.3163858.

[38] H. Lee, C.R. Ahn, N. Choi, Fine-grained occupant activity monitoring with Wi-Fi channel state information: Practical implementation of multiple receiver settings, Adv. Eng. Inform. 46 (2020) 101147, http://dx.doi.org/10.1016/j.aei.2020.101147, URL https://www.sciencedirect.com/science/article/pii/S147403462030118X.

[39] L. Jia, Y. Gu, K. Cheng, H. Yan, F. Ren, Beaware: Convolutional neural network(CNN) based user behavior understanding through WiFi channel state information, Neurocomputing 397 (2020) 457–463, http://dx.doi.org/10.1016/j.neucom.2019.09.111, URL https://www.sciencedirect.com/science/article/pii/S0925231220304124.

[40] H. Li, W. Yang, J. Wang, Y. Xu, L. Huang, WiFinger: Talk to your smart devices with finger-grained gesture, in: Proceedings of the 2016 ACM International Joint Conference on Pervasive and Ubiquitous Computing, UbiComp '16, Association for Computing Machinery, New York, NY, USA, 2016, pp. 250–261, http://dx.doi.org/10.1145/2971648.2971738.

[41] K. Ali, A.X. Liu, W. Wang, M. Shahzad, Recognizing keystrokes using WiFi devices, IEEE J. Sel. Areas Commun. 35 (5) (2017) 1175–1190, http://dx.doi.org/10.1109/JSAC.2017.2680998.

[42] Y. Zhao, R. Gao, S. Liu, L. Xie, J. Wu, H. Tu, B. Chen, Device-free secure interaction with hand gestures in WiFi-enabled IoT environment, IEEE Internet Things J. 8 (7) (2021) 5619–5631, http://dx.doi.org/10.1109/JIOT.2020.3032623.

[43] C.-L. Lin, W.-J. Chang, G.-H. Tu, Wi-Fi-based tracking of human walking for home health monitoring, IEEE Internet Things J. 9 (11) (2022) 8935–8942, http://dx.doi.org/10.1109/JIOT.2021.3118429.

[44] X. Wang, F. Li, Y. Xie, S. Yang, Y. Wang, Gait and respiration-based user identification using Wi-Fi signal, IEEE Internet Things J. 9 (5) (2022) 3509–3521, http://dx.doi.org/10.1109/JIOT.2021.3097892.

[45] J. Lv, W. Yang, D. Man, Device-free passive identity identification via WiFi signals, Sensors 17 (11) (2017) http://dx.doi.org/10.3390/s17112520, URL https://www.mdpi.com/1424-8220/17/11/2520.

[46] S. Mosleh, J.B. Coder, C.G. Scully, K. Forsyth, M.O.A. Kalaa, Monitoring respiratory motion with Wi-Fi CSI: Characterizing performance and the BreatheSmart algorithm, IEEE Access 10 (2022) 131932–131951, http://dx.doi.org/10.1109/ACCESS.2022.3230003.

[47] L. Gui, C. Ma, B. Sheng, Z. Guo, J. Cai, F. Xiao, In-home monitoring sleep turnover activities and breath rate via WiFi signals, IEEE Syst. J. 17 (2) (2023) 2355–2365, http://dx.doi.org/10.1109/JSYST.2022.3225072.

[48] A. Sharma, W. Jiang, D. Mishra, S. Jha, A. Seneviratne, Optimised CNN for human counting using spectrograms of probabilistic WiFi CSI, in: GLOBECOM 2022 - 2022 IEEE Global Communications Conference, 2022, pp. 01–06, http://dx.doi.org/10.1109/GLOBECOM48099.2022.10001169.

[49] C.M. Mesa-Cantillo, D. Sánchez-Rodríguez, I. Alonso-González, M.A. Quintana-Suárez, C. Ley-Bosch, J.B. Alonso-Hernández, A non intrusive human presence detection methodology based on channel state information of Wi-Fi networks, Sensors 23 (1) (2023) http://dx.doi.org/10.3390/s23010500, URL https://www.mdpi.com/1424-8220/23/1/500.

[50] X. Chen, Y. Zou, C. Li, W. Xiao, A deep learning based lightweight human activity recognition system using reconstructed WiFi CSI, IEEE Trans. Hum.-Mach. Syst. 54 (1) (2024) 68–78, http://dx.doi.org/10.1109/THMS.2023.3348694.

[51] J. Zhang, W. Xu, W. Hu, S.S. Kanhere, WiCare: Towards in-situ breath monitoring, in: Proceedings of the 14th EAI International Conference on Mobile and Ubiquitous Systems: Computing, Networking and Services, in: MobiQuitous 2017, Association for Computing Machinery, New York, NY, USA, 2017, pp. 126–135, http://dx.doi.org/10.1145/3144457.3144467.

[52] S. Lee, Y.-D. Park, Y.-J. Suh, S. Jeon, Design and implementation of monitoring system for breathing and heart rate pattern using WiFi signals, in: 2018 15th IEEE Annual Consumer Communications & Networking Conference, CCNC, 2018, pp. 1–7, http://dx.doi.org/10.1109/CCNC.2018.8319181.

[53] Y. Zeng, P.H. Pathak, P. Mohapatra, WiWho: WiFi-based person identification in smart spaces, in: 2016 15th ACM/IEEE International Conference on Information Processing in Sensor Networks, IPSN, 2016, pp. 1–12, http://dx.doi.org/10.1109/IPSN.2016.7460727.

[54] S.W. Shah, S.S. Kanhere, Smart user identification using cardiopulmonary activity, Pervasive Mob. Comput. 58 (2019) 101024, http://dx.doi.org/10.1016/j.pmcj.2019.05.005, URL https://www.sciencedirect.com/science/article/pii/S1574119218305145.

[55] Z. Guo, F. Xiao, B. Sheng, L. Sun, S. Yu, TWCC: A robust through-the-wall crowd counting system using ambient WiFi signals, IEEE Trans. Veh. Technol. 71 (4) (2022) 4198–4211, http://dx.doi.org/10.1109/TVT.2022.3140305.

[56] X. Liu, J. Cao, S. Tang, J. Wen, P. Guo, Contactless respiration monitoring via off-the-shelf WiFi devices, IEEE Trans. Mob. Comput. 15 (10) (2016) 2466–2479, http://dx.doi.org/10.1109/TMC.2015.2504935.

[57] A. Alzaabi, T. Arslan, N. Polydorides, Non-contact Wi-Fi sensing of respiration rate for older adults in care: A validity and repeatability study, IEEE Access 12 (2024) 6400–6412, http://dx.doi.org/10.1109/ACCESS.2024.3349700.

[58] H. Wang, D. Zhang, J. Ma, Y. Wang, Y. Wang, D. Wu, T. Gu, B. Xie, Human respiration detection with commodity WiFi devices: Do user location and body orientation matter? in: Proceedings of the 2016 ACM International Joint Conference on Pervasive and Ubiquitous Computing, UbiComp '16, Association for Computing Machinery, New York, NY, USA, 2016, pp. 25–36, http://dx.doi.org/10.1145/2971648.2971744.

[59] C. Dou, H. Huan, Full respiration rate monitoring exploiting Doppler information with commodity Wi-Fi devices, Sensors 21 (10) (2021) http://dx.doi.org/10.3390/s21103505, URL https://www.mdpi.com/1424-8220/21/10/3505.

[60] M. Liu, L. Zhang, P. Yang, L. Lu, L. Gong, Wi-run: Device-free step estimation system with commodity Wi-Fi, J. Netw. Comput. Appl. 143 (2019) 77–88, http://dx.doi.org/10.1016/j.jnca.2019.05.004, URL https://www.sciencedirect.com/science/article/pii/S108480451930164X.

[61] H. Choi, M. Fujimoto, T. Matsui, S. Misaki, K. Yasumoto, Wi-CaL: WiFi sensing and machine learning based device-free crowd counting and localization, IEEE Access 10 (2022) 24395–24410, http://dx.doi.org/10.1109/ACCESS.2022.3155812.

[62] J.C.H. Soto, I. Galdino, B.G. Gouveia, E. Caballero, V. Ferreira, D. Muchaluat-Saade, C. Albuquerque, Wi-Fi CSI-based human presence detection using DTW features and machine learning, in: 2022 IEEE Latin-American Conference on Communications, LATINCOM, 2022, pp. 1–6, http://dx.doi.org/10.1109/LATINCOM56090.2022.10000702.

[63] L. Tian, L. Chen, Z. Xu, Z.D. Chen, A people-counting and speed-estimation system using Wi-Fi signals, Sensors 21 (10) (2021) http://dx.doi.org/10.3390/s21103472, URL https://www.mdpi.com/1424-8220/21/10/3472.

[64] K. Tsubota, T. Ohhira, H. Hashimoto, Heart rate variability and body-movement extractions using Wi-Fi channel state information, in: 2023 IEEE/SICE International Symposium on System Integration, SII, 2023, pp. 1–6, http://dx.doi.org/10.1109/SII55687.2023.10039288.

[65] J. Schäfer, B.R. Barrsiwal, M. Kokhkharova, H. Adil, J. Liebehenschel, Human activity recognition using CSI information with nexmon, Appl. Sci. 11 (19) (2021) http://dx.doi.org/10.3390/app11198860, URL https://www.mdpi.com/2076-3417/11/19/8860.

[66] X. Wang, C. Yang, S. Mao, Resilient respiration rate monitoring with realtime bimodal CSI data, IEEE Sens. J. 20 (17) (2020) 10187–10198, http://dx.doi.org/10.1109/JSEN.2020.2989780.

[67] T. Kitagishi, G. Hangli, T. Michikata, N. Koshizuka, Wi-monitor: Wi-fi channel state information-based crowd counting with lightweight and low-cost IoT devices, in: A. González-Vidal, A. Mohamed Abdelgawad, E. Sabir, S. Ziegler, L. Ladid (Eds.), Internet of Things, Springer International Publishing, Cham, 2022, pp. 135–148.

[68] Y. Yin, X. Yang, J. Xiong, S.I. Lee, P. Chen, Q. Niu, Ubiquitous smartphone-based respiration sensing with Wi-Fi signal, IEEE Internet Things J. 9 (2) (2022) 1479–1490, http://dx.doi.org/10.1109/JIOT.2021.3088338.

[69] S.M. Hernandez, M. Touhiduzzaman, P.E. Pidcoe, E. Bulut, Wi-PT: Wireless sensing based low-cost physical rehabilitation tracking, in: 2022 IEEE International Conference on E-Health Networking, Application & Services, HealthCom, 2022, pp. 113–118, http://dx.doi.org/10.1109/HealthCom54947.2022.9982743.

[70] Y. Zeng, D. Wu, J. Xiong, J. Liu, Z. Liu, D. Zhang, MultiSense: Enabling multi-person respiration sensing with commodity WiFi, Proc. ACM Interact. Mob. Wearable Ubiquitous Technol. 4 (3) (2020) http://dx.doi.org/10.1145/3411816.

[71] K. Niu, F. Zhang, J. Xiong, X. Li, E. Yi, D. Zhang, Boosting fine-grained activity sensing by embracing wireless multipath effects, in: Proceedings of the 14th International Conference on Emerging Networking EXperiments and Technologies, CoNEXT '18, Association for Computing Machinery, New York, NY, USA, 2018, pp. 139–151, http://dx.doi.org/10.1145/3281411.3281425.

[72] K. Niu, F. Zhang, Y. Jiang, J. Xiong, Q. Lv, Y. Zeng, D. Zhang, WiMorse: A contactless morse code text input system using ambient WiFi signals, IEEE Internet Things J. 6 (6) (2019) 9993–10008, http://dx.doi.org/10.1109/JIOT.2019.2934904.

[73] D. Wu, R. Gao, Y. Zeng, J. Liu, L. Wang, T. Gu, D. Zhang, FingerDraw: Sub-wavelength level finger motion tracking with WiFi signals, Proc. ACM Interact. Mob. Wearable Ubiquitous Technol. 4 (1) (2020) http://dx.doi.org/10.1145/3380981.

[74] I.A. Showmik, T.F. Sanam, H. Imtiaz, Human activity recognition from Wi-Fi CSI data using principal component-based wavelet CNN, Digit. Signal Process. 138 (2023) 104056, http://dx.doi.org/10.1016/j.dsp.2023.104056, URL https://www.sciencedirect.com/science/article/pii/S1051200423001513.

[75] X. Guo, B. Liu, C. Shi, H. Liu, Y. Chen, M.C. Chuah, WiFi-enabled smart human dynamics monitoring, in: Proceedings of the 15th ACM Conference on Embedded Network Sensor Systems, SenSys '17, Association for Computing Machinery, New York, NY, USA, 2017, http://dx.doi.org/10.1145/3131672.3131692.

[76] W. Meng, X. Chen, W. Cui, J. Guo, WiHGR: A robust WiFi-based human gesture recognition system via sparse recovery and modified attention-based BGRU, IEEE Internet Things J. 9 (12) (2022) 10272–10282, http://dx.doi.org/10.1109/JIOT.2021.3122435.

[77] H. Zou, J. Yang, Y. Zhou, L. Xie, C.J. Spanos, Robust WiFi-enabled device-free gesture recognition via unsupervised adversarial domain adaptation, in: 2018 27th International Conference on Computer Communication and Networks, ICCCN, 2018, pp. 1–8, http://dx.doi.org/10.1109/ICCCN.2018.8487345.

[78] M. Kim, D. Han, J.-K.K. Rhee, Multiview variational deep learning with application to practical indoor localization, IEEE Internet Things J. 8 (15) (2021) 12375–12383, http://dx.doi.org/10.1109/JIOT.2021.3063512.

[79] X. Ma, W. Xi, X. Zhao, Z. Chen, H. Zhang, J. Zhao, Wisual: Indoor crowd density estimation and distribution visualization using Wi-Fi, IEEE Internet Things J. 9 (12) (2022) 10077–10092, http://dx.doi.org/10.1109/JIOT.2021.3119542.

[80] X. Wang, X. Wang, S. Mao, Indoor fingerprinting with bimodal CSI tensors: A deep residual sharing learning approach, IEEE Internet Things J. 8 (6) (2021) 4498–4513, http://dx.doi.org/10.1109/JIOT.2020.3026608.

[81] Y. Liu, T. Wang, Y. Jiang, B. Chen, Harvesting ambient RF for presence detection through deep learning, IEEE Trans. Neural Netw. Learn. Syst. 33 (4) (2022) 1571–1583, http://dx.doi.org/10.1109/TNNLS.2020.3042908.

[82] Y. Xiaolong, Y. Xin, X. Liangbo, X. Hao, Z. Mu, J. Qing, Sleep apnea monitoring system based on commodity WiFi devices, Comput. Mater. Contin. 69 (2) (2021) 2793–2806, http://dx.doi.org/10.32604/cmc.2021.016298, URL http://www.techscience.com/cmc/v69n2/43848.

[83] Y. Zhou, A. Zhu, C. Xu, F. Hu, Y. Li, PerUnet: Deep signal channel attention in unet for WiFi-based human pose estimation, IEEE Sens. J. 22 (20) (2022) 19750–19760, http://dx.doi.org/10.1109/JSEN.2022.3204607.

[84] M. Yang, H. Zhu, R. Zhu, F. Wu, L. Yin, Y. Yang, WiTransformer: A novel robust gesture recognition sensing model with WiFi, Sensors 23 (5) (2023) http://dx.doi.org/10.3390/s23052612, URL https://www.mdpi.com/1424-8220/23/5/2612.

[85] Q. Xu, Y. Chen, B. Wang, K.J.R. Liu, Radio biometrics: Human recognition through a wall, IEEE Trans. Inf. Forensics Secur. 12 (5) (2017) 1141–1155, http://dx.doi.org/10.1109/TIFS.2016.2647224.

[86] X. Yang, Q. Li, M. Zhou, J. Wang, Phase-calibration-based 3-D beamspace matrix pencil algorithm for indoor passive positioning and tracking, IEEE Sens. J. 23 (17) (2023) 19670–19683, http://dx.doi.org/10.1109/JSEN.2023.3295370.

[87] F. Meneghello, D. Garlisi, N.D. Fabbro, I. Tinnirello, M. Rossi, SHARP: Environment and person independent activity recognition with commodity IEEE 802.11 access points, IEEE Trans. Mob. Comput. 22 (10) (2023) 6160–6175, http://dx.doi.org/10.1109/TMC.2022.3185681.

[88] X. Li, S. Li, D. Zhang, J. Xiong, Y. Wang, H. Mei, Dynamic-MUSIC: accurate device-free indoor localization, in: Proceedings of the 2016 ACM International Joint Conference on Pervasive and Ubiquitous Computing, UbiComp '16, Association for Computing Machinery, New York, NY, USA, 2016, pp. 196–207, http://dx.doi.org/10.1145/2971648.2971665.

[89] Z. Tian, J. Wang, X. Yang, M. Zhou, WiCatch: A Wi-Fi based hand gesture recognition system, IEEE Access 6 (2018) 16911–16923, http://dx.doi.org/10.1109/ACCESS.2018.2814575.

[90] C. Chen, Y. Han, Y. Chen, H.-Q. Lai, F. Zhang, B. Wang, K.J.R. Liu, TR-BREATH: Time-reversal breathing rate estimation and detection, IEEE Trans. Biomed. Eng. 65 (3) (2018) 489–501, http://dx.doi.org/10.1109/TBME.2017.2699422.

[91] R. Yang, X. Yang, J. Wang, M. Zhou, Z. Tian, L. Li, Decimeter level indoor localization using WiFi channel state information, IEEE Sens. J. 22 (6) (2022) 4940–4950, http://dx.doi.org/10.1109/JSEN.2021.3067144.

[92] J. Liu, Y. Zeng, T. Gu, L. Wang, D. Zhang, WiPhone: Smartphone-based respiration monitoring using ambient reflected WiFi signals, Proc. ACM Interact. Mob. Wearable Ubiquitous Technol. 5 (1) (2021) http://dx.doi.org/10.1145/3448092.

[93] F. Wang, F. Zhang, C. Wu, B. Wang, K.J. Ray Liu, Passive people counting using commodity WiFi, in: 2020 IEEE 6th World Forum on Internet of Things, WF-IoT, 2020, pp. 1–6, http://dx.doi.org/10.1109/WF-IoT48130.2020.9221456.

[94] M. Atif, S. Muralidharan, H. Ko, B. Yoo, COVID-beat: a low-cost breath monitoring approach for people in quarantine during the pandemic, J. Comput. Des. Eng. 9 (3) (2022) 992–1006, http://dx.doi.org/10.1093/jcde/qwac037, arXiv: https://academic.oup.com/jcde/article-pdf/9/3/992/43796098/qwac037.pdf.

[95] W. Wang, A.X. Liu, M. Shahzad, K. Ling, S. Lu, Device-free human activity recognition using commercial WiFi devices, IEEE J. Sel. Areas Commun. 35 (5) (2017) 1118–1131, http://dx.doi.org/10.1109/JSAC.2017.2679658.

[96] H. Zou, Y. Zhou, J. Yang, C.J. Spanos, Device-free occupancy detection and crowd counting in smart buildings with WiFi-enabled IoT, Energy Build. 174 (2018) 309–322, http://dx.doi.org/10.1016/j.enbuild.2018.06.040, URL https://www.sciencedirect.com/science/article/pii/S0378778817339336.

[97] L. Guo, Z. Lu, X. Wen, S. Zhou, Z. Han, From signal to image: Capturing fine-grained human poses with commodity Wi-Fi, IEEE Commun. Lett. 24 (4) (2020) 802–806, http://dx.doi.org/10.1109/LCOMM.2019.2961890.

[98] Y. Gu, H. Yan, M. Dong, M. Wang, X. Zhang, Z. Liu, F. Ren, WiONE: One-shot learning for environment-robust device-free user authentication via commodity Wi-Fi in man–machine system, IEEE Trans. Comput. Soc. Syst. 8 (3) (2021) 630–642, http://dx.doi.org/10.1109/TCSS.2021.3056654.

[99] J. Yang, H. Zou, H. Jiang, L. Xie, Device-free occupant activity sensing using WiFi-enabled IoT devices for smart homes, IEEE Internet Things J. 5 (5) (2018) 3991–4002, http://dx.doi.org/10.1109/JIOT.2018.2849655.

[100] Y. Zhang, F. He, Y. Wang, D. Wu, G. Yu, CSI-based cross-scene human activity recognition with incremental learning, Neural Comput. Appl. 35 (17) (2023) 12415–12432, http://dx.doi.org/10.1007/s00521-023-08389-0.

[101] A. Natarajan, V. Krishnasamy, M. Singh, Design of a low-cost and device-free human activity recognition model for smart LED lighting control, IEEE Internet Things J. 11 (4) (2024) 5558–5567, http://dx.doi.org/10.1109/JIOT.2023.3308219.

[102] S.A. Shah, A. Tahir, J. Ahmad, A. Zahid, H. Pervaiz, S.Y. Shah, A.M. Abdulhadi Ashleibta, A. Hasanali, S. Khattak, Q.H. Abbasi, Sensor fusion for identification of freezing of gait episodes using Wi-Fi and radar imaging, IEEE Sens. J. 20 (23) (2020) 14410–14422, http://dx.doi.org/10.1109/JSEN.2020.3004767.

[103] R. Zhou, X. Lu, P. Zhao, J. Chen, Device-free presence detection and localization with SVM and CSI fingerprinting, IEEE Sens. J. 17 (23) (2017) 7990–7999, http://dx.doi.org/10.1109/JSEN.2017.2762428.

[104] S.D. Regani, Q. Xu, B. Wang, M. Wu, K.J.R. Liu, Driver authentication for smart car using wireless sensing, IEEE Internet Things J. 7 (3) (2020) 2235–2246, http://dx.doi.org/10.1109/JIOT.2019.2958692.

[105] L. Zhang, C. Wang, M. Ma, D. Zhang, WiDIGR: Direction-independent gait recognition system using commercial Wi-Fi devices, IEEE Internet Things J. 7 (2) (2020) 1178–1191, http://dx.doi.org/10.1109/JIOT.2019.2953488.

[106] J. Zhang, F. Wu, B. Wei, Q. Zhang, H. Huang, S.W. Shah, J. Cheng, Data augmentation and dense-LSTM for human activity recognition using WiFi signal, IEEE Internet Things J. 8 (6) (2021) 4628–4641, http://dx.doi.org/10.1109/JIOT.2020.3026732.

[107] F. Li, M.A.A. Al-qaness, Y. Zhang, B. Zhao, X. Luan, A robust and device-free system for the recognition and classification of elderly activities, Sensors 16 (12) (2016) http://dx.doi.org/10.3390/s16122043, URL https://www.mdpi.com/1424-8220/16/12/2043.

[108] Z. Fu, J. Xu, Z. Zhu, A.X. Liu, X. Sun, Writing in the air with WiFi signals for virtual reality devices, IEEE Trans. Mob. Comput. 18 (2) (2019) 473–484, http://dx.doi.org/10.1109/TMC.2018.2831709.

[109] S. Shi, S. Sigg, L. Chen, Y. Ji, Accurate location tracking from CSI-based passive device-free probabilistic fingerprinting, IEEE Trans. Veh. Technol. 67 (6) (2018) 5217–5230, http://dx.doi.org/10.1109/TVT.2018.2810307.

[110] D. Shi, J. Lu, J. Wang, L. Li, K. Liu, M. Pan, No one left behind: Avoid hot car deaths via WiFi detection, in: ICC 2020 - 2020 IEEE International Conference on Communications, ICC, 2020, pp. 1–6, http://dx.doi.org/10.1109/ICC40277.2020.9148648.

[111] Y. Wang, C. Xiu, X. Zhang, D. Yang, WiFi indoor localization with CSI fingerprinting-based random forest, Sensors 18 (9) (2018) http://dx.doi.org/10.3390/s18092869, URL https://www.mdpi.com/1424-8220/18/9/2869.

[112] Z. Wu, Q. Xu, J. Li, C. Fu, Q. Xuan, Y. Xiang, Passive indoor localization based on CSI and naive Bayes classification, IEEE Trans. Syst. Man Cybern. Syst. 48 (9) (2018) 1566–1577, http://dx.doi.org/10.1109/TSMC.2017.2679725.

[113] M. Zhou, Y. Long, W. Zhang, Q. Pu, Y. Wang, W. Nie, W. He, Adaptive genetic algorithm-aided neural network with channel state information tensor decomposition for indoor localization, IEEE Trans. Evol. Comput. 25 (5) (2021) 913–927, http://dx.doi.org/10.1109/TEVC.2021.3085906.

[114] W. Cui, B. Li, L. Zhang, Z. Chen, Device-free single-user activity recognition using diversified deep ensemble learning, Appl. Soft Comput. 102 (2021) 107066, http://dx.doi.org/10.1016/j.asoc.2020.107066, URL https://www.sciencedirect.com/science/article/pii/S1568494620310048.

[115] W. Jiang, H. Xue, C. Miao, S. Wang, S. Lin, C. Tian, S. Murali, H. Hu, Z. Sun, L. Su, Towards 3D human pose construction using WiFi, in: Proceedings of the 26th Annual International Conference on Mobile Computing and Networking, MobiCom '20, Association for Computing Machinery, New York, NY, USA, 2020, http://dx.doi.org/10.1145/3372224.3380900.

[116] Y. Ren, Z. Wang, Y. Wang, S. Tan, Y. Chen, J. Yang, GoPose: 3D human pose estimation using WiFi, Proc. ACM Interact. Mob. Wearable Ubiquitous Technol. 6 (2) (2022) http://dx.doi.org/10.1145/3534605.

[117] S. Liu, Y. Zhao, B. Chen, WiCount: A deep learning approach for crowd counting using WiFi signals, in: 2017 IEEE International Symposium on Parallel and Distributed Processing with Applications and 2017 IEEE International Conference on Ubiquitous Computing and Communications, ISPA/IUCC, 2017, pp. 967–974, http://dx.doi.org/10.1109/ISPA/IUCC.2017.00148.

[118] Y. Gu, H. Yan, X. Zhang, Y. Wang, J. Huang, Y. Ji, F. Ren, Attention-based gesture recognition using commodity WiFi devices, IEEE Sens. J. 23 (9) (2023) 9685–9696, http://dx.doi.org/10.1109/JSEN.2023.3261325.

[119] Y.-K. Cheng, R.Y. Chang, Device-free indoor people counting using Wi-Fi channel state information for internet of things, in: GLOBECOM 2017 - 2017 IEEE Global Communications Conference, 2017, pp. 1–6, http://dx.doi.org/10.1109/GLOCOM.2017.8254522.

[120] H. Zou, Y. Zhou, J. Yang, C.J. Spanos, Towards occupant activity driven smart buildings via WiFi-enabled IoT devices and deep learning, Energy Build. 177 (2018) 12–22, http://dx.doi.org/10.1016/j.enbuild.2018.08.010, URL https://www.sciencedirect.com/science/article/pii/S037877881831329X.

[121] R. Zhou, M. Hao, X. Lu, M. Tang, Y. Fu, Device-free localization based on CSI fingerprints and deep neural networks, in: 2018 15th Annual IEEE International Conference on Sensing, Communication, and Networking, SECON, 2018, pp. 1–9, http://dx.doi.org/10.1109/SAHCN.2018.8397121.

[122] B. Zhao, D. Zhu, T. Xi, C. Jia, S. Jiang, S. Wang, Convolutional neural network and dual-factor enhanced variational Bayes adaptive Kalman filter based indoor localization with Wi-Fi, Comput. Netw. 162 (2019) 106864, http://dx.doi.org/10.1016/j.comnet.2019.106864, URL https://www.sciencedirect.com/science/article/pii/S1389128618311691.

[123] H. Chen, Y. Zhang, W. Li, X. Tao, P. Zhang, ConFi: Convolutional neural networks based indoor Wi-Fi localization using channel state information, IEEE Access 5 (2017) 18066–18074, http://dx.doi.org/10.1109/ACCESS.2017.2749516.

[124] Y. Zhou, H. Huang, S. Yuan, H. Zou, L. Xie, J. Yang, MetaFi++: WiFi-enabled transformer-based human pose estimation for metaverse avatar simulation, IEEE Internet Things J. (2023) http://dx.doi.org/10.1109/JIOT.2023.3262940, 1–1.

[125] M. Schulz, D. Wegemer, M. Hollick, Nexmon: The C-based firmware patching framework, 2017, URL https://nexmon.org.

[126] F. Gringoli, M. Schulz, J. Link, M. Hollick, Free your CSI: A channel state information extraction platform for modern Wi-Fi chipsets, in: Proceedings of the 13th International Workshop on Wireless Network Testbeds, Experimental Evaluation & Characterization, WiNTECH '19, 2019, pp. 21–28.

[127] F. Gringoli, M. Cominelli, A. Blanco, J. Widmer, AX-CSI: Enabling CSI extraction on commercial 802.11ax Wi-Fi platforms, in: Proceedings of the 15th ACM Workshop on Wireless Network Testbeds, Experimental Evaluation & CHaracterization, WiNTECH '21, Association for Computing Machinery, New York, NY, USA, 2021, pp. 46–53, http://dx.doi.org/10.1145/3477086.3480833.

[128] X. Jiao, W. Liu, M. Mehari, M. Aslam, I. Moerman, Openwifi: a free and open-source IEEE802.11 SDR implementation on SoC, in: 2020 IEEE 91st Vehicular Technology Conference, VTC2020-Spring, 2020, pp. 1–2, http://dx.doi.org/10.1109/VTC2020-Spring48590.2020.9128614.

[129] C. Chen, H. Song, Q. Li, F. Meneghello, F. Restuccia, C. Cordeiro, Wi-Fi sensing based on IEEE 802.11bf, IEEE Commun. Mag. 61 (1) (2023) 121–127, http://dx.doi.org/10.1109/MCOM.007.2200347.

[130] T.L. Floyd, Dispositivos Electrónicos, eighth ed., Pearson Education, México, 2008, pp. 756–760.

[131] R. Pearson, Outliers in process modeling and identification, IEEE Trans. Control Syst. Technol. 10 (1) (2002) 55–63, http://dx.doi.org/10.1109/87.974338.

[132] H.C. Chen, S.W. Chen, A moving average based filtering system with its application to real-time QRS detection, in: Computers in Cardiology, 2003, 2003, pp. 585–588, http://dx.doi.org/10.1109/CIC.2003.1291223.

[133] R.W. Schafer, What is a Savitzky-Golay filter? [lecture notes], IEEE Signal Process. Mag. 28 (4) (2011) 111–117, http://dx.doi.org/10.1109/MSP.2011.941097.

[134] R. Schmidt, Multiple emitter location and signal parameter estimation, IEEE Trans. Antennas and Propagation 34 (3) (1986) 276–280, http://dx.doi.org/10.1109/TAP.1986.1143830.

[135] M. Weeks, Digital Signal Processing using MATLAB and Wavelets, Infinity Science Press, 2007, pp. 85–112.

[136] R.M. Howard, Principles of Random Signal Analysis and Low Noise Design: The Power Spectral Density and Its Applications, John Wiley & Sons, 2004, pp. 1–2.

[137] C.S. Burrus, R.A. Gopinath, H. Guo, Wavelets and Wavelet Transforms, Houston ed., Vol. 98, Rice University, 1998.

[138] P. Bentley, J. McDonnell, Wavelet transforms: an introduction, Electron. Commun. Eng. J. 6 (4) (1994) 175–186, http://dx.doi.org/10.1049/ecej:19940401.

[139] I. Daubechies, Ten Lectures on Wavelets, SIAM, 1992.

[140] G. Tzanetakis, G. Essl, P. Cook, Audio analysis using the discrete wavelet transform, in: Proceedings of the Conference in Acoustics and Music Theory Applications, 2001, pp. 318–323.

[141] I.T. Jolliffe, J. Cadima, Principal component analysis: a review and recent developments, Phil. Trans. R. Soc. A 374 (2065) (2016) 20150202, http://dx.doi.org/10.1098/rsta.2015.0202.

[142] Q. Tan, C. Han, L. Sun, J. Guo, H. Zhu, A CSI frequency domain fingerprint-based method for passive indoor human detection, in: 2018 17th IEEE International Conference on Trust, Security and Privacy in Computing and Communications/ 12th IEEE International Conference on Big Data Science and Engineering, TrustCom/BigDataSE, 2018, pp. 1832–1837, http://dx.doi.org/10.1109/TrustCom/BigDataSE.2018.00277.

[143] F. Zhang, C. Chen, B. Wang, K.J.R. Liu, WiSpeed: A statistical electromagnetic approach for device-free indoor speed estimation, IEEE Internet Things J. 5 (3) (2018) 2163–2177, http://dx.doi.org/10.1109/JIOT.2018.2826227.

[144] T. Hang, Y. Zheng, K. Qian, C. Wu, Z. Yang, X. Zhou, Y. Liu, G. Chen, WiSH: WiFi-based real-time human detection, Tsinghua Sci. Technol. 24 (5) (2019) 615–629, http://dx.doi.org/10.26599/TST.2018.9010091.

[145] J. Wang, J. Xiong, H. Jiang, K. Jamieson, X. Chen, D. Fang, C. Wang, Low human-effort, device-free localization with fine-grained subcarrier information, IEEE Trans. Mob. Comput. 17 (11) (2018) 2550–2563, http://dx.doi.org/10.1109/TMC.2018.2812746.

[146] E. Kim, S. Helal, D. Cook, Human activity recognition and pattern discovery, IEEE Pervasive Comput. 9 (1) (2010) 48–53, http://dx.doi.org/10.1109/MPRV.2010.7.

[147] L. Guo, L. Wang, C. Lin, J. Liu, B. Lu, J. Fang, Z. Liu, Z. Shan, J. Yang, S. Guo, Wiar: A public dataset for Wifi-based activity recognition, IEEE Access 7 (2019) 154935–154945, http://dx.doi.org/10.1109/ACCESS.2019.2947024.

[148] Z. Yang, Y. Zhang, G. Zhang, Y. Zheng, Widar 3.0: WiFi-based activity recognition dataset, 2020, http://dx.doi.org/10.21227/7znf-qp86.

[149] M. Atif, S. Muralidharan, H. Ko, B. Yoo, Wi-ESP—A tool for CSI-based device-free Wi-Fi sensing (DFWS), J. Comput. Des. Eng. (2020) qwaa048, http://dx.doi.org/10.1093/jcde/qwaa048, arXiv:https://academic.oup.com/jcde/article-pdf/doi/10.1093/jcde/qwaa048/33217218/qwaa048.pdf.

[150] S. Blandino, T. Ropitault, C.R.C.M. da Silva, A. Sahoo, N. Golmie, IEEE 802.11bf DMG sensing: Enabling high-resolution mmwave Wi-Fi sensing, IEEE Open J. Veh. Technol. 4 (2023) 342–355, http://dx.doi.org/10.1109/OJVT.2023.3237158.

[151] M. Cominelli, F. Gringoli, R. Lo Cigno, AntiSense: Standard-compliant CSI obfuscation against unauthorized Wi-Fi sensing, Comput. Commun. 185 (2022) 92–103, http://dx.doi.org/10.1016/j.comcom.2021.12.019, URL https://www.sciencedirect.com/science/article/pii/S0140366421004916.

[152] X. Meng, J. Zhou, X. Liu, X. Tong, W. Qu, J. Wang, Secur-Fi: A secure wireless sensing system based on commercial Wi-Fi devices, in: IEEE INFOCOM 2023 - IEEE Conference on Computer Communications, 2023, pp. 1–10, http://dx.doi.org/10.1109/INFOCOM53939.2023.10229055.

[153] M. Cominelli, F. Gringoli, R. Lo Cigno, On the properties of device-free multi-point CSI localization and its obfuscation, Comput. Commun. 189 (2022) 67–78, http://dx.doi.org/10.1016/j.comcom.2022.03.011, URL https://www.sciencedirect.com/science/article/pii/S014036642200086X.

[154] X. Jiao, M. Mehari, W. Liu, M. Aslam, I. Moerman, openwifi CSI fuzzer for authorized sensing and covert channels, in: Proceedings of the 14th ACM Conference on Security and Privacy in Wireless and Mobile Networks, WiSec '21, Association for Computing Machinery, New York, NY, USA, 2021, pp. 377–379, http://dx.doi.org/10.1145/3448300.3468255.

[155] L. Ghiro, M. Cominelli, F. Gringoli, R. Lo Cigno, Wi-Fi localization obfuscation: An implementation in openwifi, Comput. Commun. 205 (2023) 1–13, http://dx.doi.org/10.1016/j.comcom.2023.03.026, URL https://www.sciencedirect.com/science/article/pii/S0140366423001111.